Imbalanced Sparse Canonical Correlation Analysis

Wenjia Wang
The Statistical and Applied Mathematical Sciences Institute
Durham, NC, U.S.A.
wenjia.wang234@duke.edu

Yi-Hui Zhou
Department of Biological Sciences
North Carolina State University, Raleigh, NC, U.S.A.
yihui_zhou@ncsu.edu

Abstract

Classical canonical correlation analysis (CCA) requires matrices to be low dimensional, i.e. the number of features cannot exceed the sample size. Recent developments in CCA have mainly focused on the high-dimensional setting, where the number of features in both matrices under analysis greatly exceeds the sample size. However, these approaches make considerable sparsity assumptions and impose penalties that may be unnecessary for some datasets. We consider an imbalanced setting that is commonly encountered, where one matrix is high dimensional and the other is low dimensional. We provide an explicit link between sparse multiple regression with sparse canonical correlation analysis, and an efficient algorithm that exploits the imbalanced data structure and estimates multiple canonical pairs rather than sequentially. We provide theoretical results on the consistency of canonical pairs. Simulation results and the analysis of several real datasets support the improved performance of the proposed approach.

1 Introduction

Canonical correlation analysis (CCA) is a widely used method to determine the relationship between two sets of variables. In CCA, the objective is to find a linear combination of variables from each set of variables such that the correlation is maximized. The vectors consist of coefficients from each linear combination is called canonical pairs. Originally proposed by Hotelling (1936), CCA has been applied to numerous problems, including those of large scale. In large scale problems, including genomic studies, researchers are often faced with high dimensional data. For example, Chen et al. (2012) studied the association between nutrient intake and human gut microbiome composition, and Wang et al. (2015) studied the group interactions among genes. Projects such as GTEx (Aguet et al., 2019) also provide rich datasets for which CCA might be used to identify important genetic modules relevant to

disease. In these works, classical CCA cannot be used to analyze the high dimensional data, where the number of variables exceeds the number of observations.

To study the relationship between two sets of high dimensional variables, many extensions of classical CCA have been proposed. One popular approach, sparse canonical correlation analysis, imposes sparse structure on the canonical vectors. An incomplete list of sparse CCA methods is Parkhomenko et al. (2009); Witten and Tibshirani (2009); Waaijenborg et al. (2008); Lê Cao et al. (2009); Witten et al. (2009); Chen et al. (2012), and references therein. In these works, the dimensions of the two variables being compared are both high.

In some cases, the dimensions of the two variables can be quite different. For example, in the application to gut microbiome data analysis (Chen et al., 2012), the dimensions of two variables were 214 and 40, while the sample size was 99. Such datasets have a partially low dimensional structure, that is, the dimension of one variable is larger than the sample size, and the other one has dimension lower than the sample size. The sparse canonical correlation analysis does not utilize the partially low dimensional structure, and may provide biased canonical pairs of canonical vectors.

In order to estimate the canonical pairs in the problems with partially low dimensional structure, in this work, we propose *imbalanced sparse canonical correlation analysis*. Specifically, we link sparse multiple regression with sparse canonical correlation analysis, and apply Lasso regularization to the estimation of the canonical pairs. We propose an efficient algorithm to provide K canonical pairs simultaneously for $K \geq 1$. This advantage significantly differentiates our method from other sparse canonical correlation analysis methods, which usually estimate multiple canonical pairs sequentially. Importantly, we also provide theoretical guarantees on the consistency of estimated canonical pairs.

We note that the relationship between multiple regression and CCA has been considered previously. In Glahn (1968), multiple regression was considered as be a special case of CCA, but the high dimensional situation was not considered. Lutz and Eckert (1994) analyzed the relationship between multiple regression and CCA via eigenstructure. Yamamoto et al. (2008) applied CCA to multivariate regression. Song et al. (2016) assumed that the responses have a linear relationship with some underlying signals. However, we are not aware of any works that apply sparse multiple regression to canonical correlation analysis.

The rest of this paper is arranged as follows. In Section 2, we introduce classical canonical correlation analysis and sparse canonical correlation analysis. We propose an imbalanced sparse canonical correlation analysis approach, with attendant theoretical properties. In Section 3, we compare the imbalanced sparse canonical correlation analysis to existing methods, and highlight the potential advantages and importance of the proposed method. In Section 4, we conduct numeric simulation studies. In Section 5, we apply imbalanced sparse canonical correlation analysis and competing methods to three applied problems, including human gut microbiome data, GTEx thyroid imaging/expression data, and GTEx liver genotype/expression data. A Discussion with conclusions is provided in Section 6. Technical proofs are provided in the Appendix.

2 Background and Proposed Methods

In this section, we provide a brief introduction to classical canonical correlation analysis and sparse canonical correlation analysis, propose imbalanced sparse canonical correlation analysis, and study its theoretical properties.

2.1 Classical CCA and Sparse CCA

Suppose we are interested in studying the correlation between two sets of random variables $x = (x_1, ..., x_p)^T \in \mathbb{R}^p$ and $y = (y_1, ..., y_d)^T \in \mathbb{R}^d$. The goal of canonical correlation analysis (CCA) is to find $a_1 \in \mathbb{R}^d$ and $b_1 \in \mathbb{R}^p$ such that (a_1, b_1) is the solution to

$$\max_{a \in \mathbb{R}^d} \operatorname{corr}(a^T y, b^T x). \tag{1}$$

Without loss of generality, we assume x and y have mean zero, for otherwise we can shift the mean. Let Σ_{xx} and Σ_{yy} be the covariance matrix of x and y, respectively. Let Σ_{xy} be the covariance matrix between x and y. The optimization problem (1) is the same as

$$\max_{a \in \mathbb{R}^d, b \in \mathbb{R}^p} \frac{a^T \Sigma_{yx} b}{\sqrt{a^T \Sigma_{yy}} a \sqrt{b^T \Sigma_{xx}} b}.$$
 (2)

The solution to (2), denoted by a_1 and b_1 , are called the first pair of canonical vectors, and the new variables $x'_1 = a_1^T x$ and $y'_1 = b_1^T y$ are called the first pair of canonical variables (Mardia et al., 1979). Once the (k-1)-th pair of canonical vectors a_{k-1} and b_{k-1} are obtained, the k-th pair of canonical vectors is the solution to the optimization problem

$$\max_{a \in \mathbb{R}^d, b \in \mathbb{R}^p} \frac{a^T \Sigma_{yx} b}{\sqrt{a^T \Sigma_{yy} a \sqrt{b^T \Sigma_{xx} b}}}$$
s.t.
$$a^T \Sigma_{yy} a_l = 0, b^T \Sigma_{xx} b_l = 0, 1 \le l \le k - 1,$$
(3)

for $k = 2, ..., \min\{d, p\}$.

By basic matrix computation, one can obtain that the solution a_k to the optimization problem (3) is the k-th eigenvector of

$$\Sigma_{yy}^{-1}\Sigma_{yx}\Sigma_{xx}^{-1}\Sigma_{xy},\tag{4}$$

and b_k is proportional to

$$\sum_{xx}^{-1} \sum_{xy} a_k. \tag{5}$$

Note that the solution to (3) is not unique, because for any constant $C \in \mathbb{R}$ and $C \neq 0$, if (a_k, b_k) is the solution to (3), then so is (Ca_k, Cb_k) . Therefore, we restrict the norms of a_k and b_k such that $||a_k||_2 = ||b_k||_2 = 1$, and the first nonzero element of a_k (b_k) is positive to make the solution to (3) unique, where $||\cdot||_2$ is the Euclidean norm.

Let $X_i, Y_i, i = 1, ..., n$ be observations, where $X_i = (x_{i1}, ..., x_{ip})^T$ and $Y_i = (y_{i1}, ..., y_{id})^T$. Let $X = (X_1, ..., X_n)$ and $Y = (Y_1, ..., Y_n)$ be the sample matrices. In classical CCA, the covariance matrices Σ_{xx} , Σ_{yy} , and Σ_{yx} are replaced by XX^T/n , YY^T/n , and YX^T/n , respectively (González et al., 2008). This approach does not work if the dimension of x or y is larger than the sample size n, because XX^T/n or YY^T/n is singular. To address the case when p or d is larger than n, several modifications of the classical CCA have been proposed. One widely used method, sparse canonical correlation analysis, restricts the estimated canonical vectors to be sparse. In Parkhomenko et al. (2009), the sparse canonical vectors are obtained by an algorithm where a threshold is used to control the sparsity of canonical vectors. Another way to obtain the sparse canonical vectors is via regularization (Witten and Tibshirani, 2009; Witten et al., 2009; Chen et al., 2012), where the k-th pair of canonical vectors is obtained by solving

$$\max_{a,b} \frac{1}{n} a^T Y X^T b$$
s.t. $||a||_2 \le 1, ||b||_2 \le 1, P_1(a) \le c_1, P_2(b) \le c_2, a^T Y Y^T a_l = 0, b^T X X^T b_l = 0, 1 \le l < k,$
(6)

where P_1 and P_2 are two convex penalty functions, and c_1 and c_2 are two constants. In this model, the sparsity is imposed on the canonical vectors by using different penalty functions. In Section 3, we will provide a more detailed introduction to sparse canonical correlation analysis.

2.2 Imbalanced Sparse CCA

In some cases, the dimensions of x and y are very different. Without loss of generality for our application domain, we assume the dimension of x is much larger than the sample size, while the dimension of y is relatively small. In this work, we propose *imbalanced sparse canonical correlation analysis*, which can be used to estimate the canonical vectors under the the setting $p \gg n > d$. This imbalance allows us to use the low dimensional structure of y to compute canonical vectors efficiently. One may still use sparse CCA (6) in this setting to estimate the canonical vectors, but may lose some efficiency or incur substantial bias, as we will see in the numerical studies. In contrast with existing sparse CCA methods (6), we do not approach the problem directly as in terms of the CCA correlation maximization. First, we establish a relationship between multivariate regression and CCA. This relationship allows us to apply existing methodologies from regression, which makes the algorithm of estimating canonical vectors more efficient.

Consider a multivariate linear regression on y with variables x,

$$y = B_* x + \epsilon_y, \tag{7}$$

where $B_* \in \mathbb{R}^{d \times p}$ is the coefficient matrix. The variable ϵ_y is the residual, and $\mathbb{E}(\epsilon_y^T B_* x) = 0$. With the relationship (7), we can compute the covariance matrices Σ_{xy} and Σ_{yy} by

$$\Sigma_{xy} = \Sigma_{xx} B_*^T, \quad \Sigma_{yy} = B_* \Sigma_{xx} B_*^T + \Sigma_{\epsilon_y \epsilon_y}, \tag{8}$$

where the second equality follows from $\mathbb{E}(\epsilon_y^T B_* x) = 0$. By the results in classical CCA, the first canonical vector of the k-th pair of canonical vectors a_k is the k-th eigenvector of

$$\Sigma_{yy}^{-1} \Sigma_{yx} \Sigma_{xx}^{-1} \Sigma_{xy} = \Sigma_{yy}^{-1} B_* \Sigma_{xx} B_*^T, \tag{9}$$

where the equality is because of (8). The second canonical vector b_k is proportional to

$$\Sigma_{xx}^{-1} \Sigma_{xy} a_k = \Sigma_{xx}^{-1} \Sigma_{xx} B_*^T a_k = B_*^T a_k.$$
 (10)

Note that in (9) and (10), we do not need to compute Σ_{xx}^{-1} . Therefore, we avoid the problem that XX^T/n is singular. Thus, if B_* is known, we can replace Σ_{xx} and Σ_{yy} in (9) by XX^T/n and YY^T/n , respectively, to estimate the canonical vectors.

In practice, B_* is rarely known. Therefore, we need to estimate B_* in order to use (9) and (10) to obtain the canonical vectors. Note that $B_* \in \mathbb{R}^{d \times p}$ with $p \gg d$. One natural idea is to assume the coefficient matrix B_* has some sparse structure, and to use the elementwise l_1 penalty as a regularization as in Lasso (Tibshirani, 1996). To be specific, let \hat{B} be an estimator of B_* . We compute \hat{B} by the following optimization problem

$$\min_{B \in \mathbb{R}^{d \times p}} \sum_{i=1}^{n} \|Y_i - BX_i\|_2^2 + \lambda_1 \|B\|_{F_1}, \tag{11}$$

where

$$||B||_{F_1} = \sum_{j=1}^d ||\beta_j||_1,$$

for $B = (\beta_1, ..., \beta_d)^T$, $\|\cdot\|_1$ is the l_1 norm, and $\lambda_1 > 0$ is a tuning parameter. Noting that (11) can be rewritten as

$$\sum_{i=1}^{n} \|Y_i - BX_i\|_2^2 + \lambda_1 \|B\|_{F_1}$$

$$= \sum_{i=1}^{n} \sum_{j=1}^{d} (y_{ij} - \beta_j^T X_i)^2 + \lambda_1 \sum_{j=1}^{d} \|\beta_j\|_1$$

$$= \sum_{j=1}^{d} \left(\sum_{i=1}^{n} (y_{ij} - \beta_j^T X_i)^2 + \lambda_1 \|\beta_j\|_1 \right),$$

we can decompose (11) into d Lasso problems,

$$\min_{\beta_j} \sum_{i=1}^n (y_{ij} - \beta_j^T X_i)^2 + \lambda_1 \|\beta_j\|_1$$
 (12)

for j = 1, ..., d. Let $\hat{\beta}_j$ be the solution to (12), and $\hat{B} = (\hat{\beta}_1, ..., \hat{\beta}_d)^T$. Therefore, \hat{B} is an estimator of B_* . By replacing B_* , Σ_{xx} and Σ_{yy} in (9) and (10) with \hat{B} , XX^T/n and YY^T/n , respectively, we can obtain the k-th pair of estimated canonical vectors \hat{a}_k and \hat{b}_k as follows. The first estimated canonical vector \hat{a}_k is the k-th eigenvector of

$$(YY^T)^{-1}\hat{B}X(\hat{B}X)^T$$
,

Algorithm 1 Imbalanced sparse CCA

- 1: **Input:** Observed data X and Y.
- 2: Solve (12) for j = 1, ..., d to obtain the estimated coefficient matrix B.
- 3: Calculate the eigenvectors of $(YY^T)^{-1}\hat{B}X(\hat{B}X)^T$. The k-th eigenvector \hat{a}_k is the first estimated canonical vector in the k-th pair of estimated canonical vectors. The second estimated canonical vector is $\hat{b}'_k = \hat{B}^T \hat{a}_k$.
- 4: Normalize \hat{b}'_k as \hat{b}_k such that $||\hat{b}_k||_2 = 1$.
- 5: **Output:** The k-th pair of estimated canonical vectors \hat{a}_k and \hat{b}_k .

and the second canonical vector \hat{b}_k is proportional to

$$\hat{B}^T \hat{a}_k$$
.

Algorithm 1 describes the procedure to obtain the k-th pair of estimated canonical vectors. Compared with existing methods, the proposed algorithm has the following advantages. First, we do not use any iteration in our algorithm, except in solving Lasso, which has been well studied and optimized in the literature (Friedman et al., 2010). Therefore, Algorithm 1 is efficient, since we assume d is small. Second, in Algorithm 1, it can be seen that we obtain multiple pairs of estimated canonical vectors simultaneously. This implies that we do not need to estimate multiple pairs of canonical vectors sequentially. In particular, if one is only interested in the k-th pair of canonical vectors, one does not need to know l-th canonical vectors for l < k. We will discuss the comparison between imbalanced sparse CCA and existing methodologies in greater detail in Section 3.

2.3 Theoretical Properties

In this subsection, we present theoretical results of imbalanced sparse CCA. We mainly focus on the consistency of the estimated canonical vectors. We first introduce some technical assumptions. In the rest of this work, we will use the following definitions. For notational simplicity, we will use $C, C', C_1, C_2, ...$ and $K, K_1, K_2, ...$ to denote the constants, of which the values can change from line to line. For two positive sequences s_n and t_n , we write $s_n \approx t_n$ if, for some constants C, C' > 0, $C \leq s_n/t_n \leq C'$. Similarly, we write $s_n \gtrsim t_n$ if $s_n \geq Ct_n$ for some constant C > 0, and $s_n \lesssim t_n$ if $s_n \leq C't_n$ for some constant C' > 0.

The first assumption is the regularity conditions on the covariance matrices Σ_{xx} and $\Sigma_{\epsilon_y \epsilon_y}$.

Assumption 1. Let $\lambda_{\max}(U)$ and $\lambda_{\min}(U)$ be the maximum and minimum eigenvalues of matrix U, respectively. Assume there exist positive constants K_1 and K_2 such that

$$K_1 \leq \min \left\{ \lambda_{\min}(\Sigma_{xx}), \lambda_{\min}(\Sigma_{\epsilon_y \epsilon_y}) \right\} \leq \max \left\{ \lambda_{\max}(\Sigma_{xx}), \lambda_{\max}(\Sigma_{\epsilon_y \epsilon_y}) \right\} \leq K_2.$$

Assumption 1 assures that the eigenvalues of the covariance matrix are bounded, which is a typical condition for the high dimensional analysis; see Gao et al. (2017); Chen et al. (2013) for example.

The second assumption is on the coefficient matrix B_* .

Assumption 2. Suppose B_* satisfies $\sigma_{\max}(B_*) \leq K$ for some constant K > 0, where $\sigma_{\max}(B_*)$ is the maximum singular value of B_* .

As a simple consequence of Assumptions 1 and 2, the eigenvalues of the covariance matrix Σ_{yy} are bounded above by a constant, and bounded below from zero, as shown in the following proposition.

Proposition 1. Suppose Assumptions 1 and 2 hold. Then there exist positive constants K_1 and K_2 such that

$$K_1 \le \lambda_{\min}(\Sigma_{yy}) \le \lambda_{\max}(\Sigma_{yy}) \le K_2.$$

The following assumption is on the matrix $\Sigma_{yy}^{-1} B_* \Sigma_{xx} B_*^T$.

Assumption 3. Let $\Gamma = \Sigma_{yy}^{-1} B_* \Sigma_{xx} B_*^T$. Suppose the Schur decomposition of Γ with respect to k-th eigenvalue and eigenvector is

$$Q_k^T \Gamma Q_k = \left[\begin{array}{cc} \lambda_k & v_k^T \\ 0 & T_k \end{array} \right],$$

where $Q_k = [q_k, Q_k'] \in \mathbb{R}^{p \times p}$ is orthogonal (thus, q_k is the k-th eigenvector of Γ). Assume there exist some constants $\sigma_1 > 0$ and K > 0 such that for all k = 1, ..., d, $\sigma_k = \sigma_{\min}(T_k - \lambda_k I) > \sigma_1$ and $\|v_k\|_2 < K$, where $\sigma_{\min}(T_k - \lambda_k I)$ is the minimum singular value of $T_k - \lambda_k I$.

Assumption 3 imposes the conditions on the matrix $\Sigma_{yy}^{-1}B_*\Sigma_{xx}B_*^T$, which ensures the numerical stability of the calculation of the eigenvectors of $\Sigma_{yy}^{-1}B_*\Sigma_{xx}B_*^T$. The singular value condition $\sigma_{\min}(T_k - \lambda_k I) > \sigma_1$ is necessary because if λ_k is a nondefective, repeated eigenvalue of Γ , there exist infinitely many of eigenvectors corresponding to λ_k , thus the consistency of eigenvectors cannot hold. Roughly speaking, Assumption 3 requires that the eigenvalues of $\Sigma_{yy}^{-1}B_*\Sigma_{xx}B_*^T$ are well separated.

The next assumption is related to the tail behaviors of variables x, y, and ϵ_y .

Definition 1. A vector $v = (v_1, ..., v_p)^T$ is sub-Gaussian, if there exist positive constants K and σ such that

$$K^2(\mathbb{E}e^{v_i^2/K^2} - 1) \le \sigma^2$$

holds for all $i \in \{1, ..., p\}$.

Assumption 4. The random variables x, y, and ϵ_y are all sub-Gaussian. Furthermore, ϵ_y is independent of x.

The sub-Gaussian assumption in Assumption 4 is also typical in high dimensional analysis. As a simple example, $x \sim N(0, \Sigma_{xx})$ and $y \sim N(0, \Sigma_{yy})$ are sub-Gaussian, where $N(0, \Sigma)$ is a multivariate normal distribution with mean zero and covariance matrix Σ . The independence assumption of ϵ_y and x is slightly stronger than the condition $\mathbb{E}(\epsilon_y^T A x) = 0$, which can be always done by projection of y onto x, if x and y are normally distributed.

Under Assumptions 1-4, we have the following consistency results, as shown in Theorem 1. The proof of Theorem 1 can be found in Appendix C.

Theorem 1. Let $B_* = (\beta_1^*, ..., \beta_d^*)^T$ with $\beta_k^* = (\beta_{k1}^*, ..., \beta_{kp}^*)^T$. Suppose Assumptions 1-4 hold. Furthermore, assume $\max_k \operatorname{supp}(\beta_k^*) = s^*$, $n^{-1/2}s^* \log p = o(1)$, and $\lambda_1 \asymp \sqrt{n \log p}$, where $\operatorname{supp}(\beta_k^*) = \operatorname{card}(\{j | \beta_{kj}^* \neq 0\})$ and $\operatorname{card}(A)$ is the cardinality of set A. Then with probability at least $1 - C_1 d^3/p$,

$$\max\{\|a_k - \hat{a}_k\|_2, \|b_k - \hat{b}_k\|_2\} \lesssim \sqrt{d(d+s^*)\log p/n},\tag{13}$$

for all k = 1, ..., d, where C_1 is a positive constant not depending on n.

In Theorem 1, it can be seen that if d is small, then imbalanced sparse CCA can provide consistent estimators of canonical vectors, under the high dimensional settings with respect to the second random variable.

3 Comparison with Existing Methods

In this section, we first review some existing methods, and then compare imbalanced sparse CCA with these existing methods. As introduced in Section 2.1, when the dimension of x or y is larger than the sample size n, the classical CCA cannot be directly applied. One naive method to estimate the canonical vectors is to add diagonal matrices $\mu_Y I_d$ and $\mu_X I_p$ with $\mu_Y, \mu_X > 0$ such that the estimated covariance matrix $\Sigma_{YY} + \mu_Y I_d$ and $\Sigma_{XX} + \mu_X I_p$ are invertible, where I_d and I_p are two identity matrices of size d and p, respectively, $\Sigma_{YY} = YY^T/n$, and $\Sigma_{XX} = XX^T/n$. Following the terminology in spatial statistics (Stein, 1999) and computer experiments (Peng and Wu, 2014), we call μ_X and μ_Y "nugget" parameters, and call the corresponding method CCA with a nugget parameter. CCA with a nugget parameter provides the first canonical vector a_μ as an eigenvector of

$$(\Sigma_{YY} + \mu_Y I_d)^{-1} \Sigma_{YX} (\Sigma_{XX} + \mu_X I_p)^{-1} \Sigma_{XY}, \tag{14}$$

and the second canonical vector b_{μ} is proportional to

$$(\Sigma_{XX} + \mu_X I_p)^{-1} \Sigma_{XY} a, \tag{15}$$

where $\Sigma_{XY} = XY^T/n$ and $\Sigma_{YX} = \Sigma_{XY}^T$. Although using a nugget parameter enables the matrix inverse, it may produce non-sparse canonical vectors, which may hard to interpret. If the dimension of Y is not large, then the non-sparse canonical vector a_{μ} is reasonable. However, since the dimension of X is large, it is desirable to have a sparse canonical vector b_{μ} , and CCA with a nugget parameter may not be appropriate to use.

Many other approaches to generalize classical CCA to high dimensional settings have been proposed. In these works, thresholding or regularization is introduced into the optimization problem (1). For example, Parkhomenko et al. (2009, 2007); Waaijenborg et al. (2008) introduced a soft-thersholding for each element of canonical vectors. Therefore, elements with small absolute value are forced to be zero, and a sparse solution is obtained. Chen et al. (2013) introduced iterative thresholding to estimate the canonical vectors, and showed that the consistency of estimated canonical vectors holds under the assumptions that Σ_{xx} and Σ_{yy} (or the inverses of them) are sparse. Tenenhaus and Tenenhaus (2011) proposed a regularized generalized CCA, where the constraint on canonical vectors are changed to be

 $\tau_1 a^T \Sigma_{XX} a + (1 - \tau_1) \|a\|_2 = 1$ and $\tau_2 b^T \Sigma_{YY} b + (1 - \tau_2) \|b\|_2 = 1$, where $\tau_1, \tau_2 \in [0, 1]$ are two tuning parameters.

Regularization-based sparse CCA usually has the form (6). This method was proposed by Witten et al. (2009), and has been extended by Witten and Tibshirani (2009). An algorithm based on Witten and Tibshirani (2009) has been proposed by Lee et al. (2011b). In Waaijenborg et al. (2008), the elastic net was also used to obtain sparsity of the estimated canonical vectors. Chen et al. (2012) modified sparse CCA as in Witten and Tibshirani (2009) by adding a structure based constraint to the canonical vectors. Gao et al. (2017) proposed a method called convex program with group-Lasso refinement, which is a two-stage method based on group Lasso, and they proved the consistency of estimated canonical variables.

Another type of sparse CCA methods is via reformulation. In Hardoon and Shawe-Taylor (2011), it was shown that based on a primal-dual framework, (2) is equivalent to the following problem

$$\min_{w,e} \|X^T w - Y^T Y e\|_2^2, \tag{16}$$

subject to $||Y^TYe||_2^2 = 1$, in the sense that (w, e) is the solution to (16) if and only if there exists μ, γ such that $(\mu w, \gamma Y e)$ is the solution to (2). Then by imposing l_1 regularization on w and e, sparse canonical vectors can be obtained. Recent work by Mai and Zhang (2019) reformulated (6) into a constrained quadratic optimization problem, and proposed an iterative penalized least squares algorithm to solve the optimization problem. Theoretical guarantees on the consistency of the estimated canonical vectors were also presented in Mai and Zhang (2019).

Our proposed method, imbalanced sparse CCA, is substantially different from all existing methods from the following perspectives. First, the scope of imbalanced sparse CCA is different from sparse CCA. In imbalanced sparse CCA, we target the estimation of canonical vectors under the settings $d < n \ll p$. Although the case of $d < n \ll p$ can be covered by the methods mentioned above, these methods do not utilize the partially low dimensional structure. Imbalanced sparse CCA, on the other hand, utilizes the low dimensional structure. Many methods mentioned above need to solve Lasso in each iteration of the algorithm, until the algorithm converges; see Mai and Zhang (2019); Waaijenborg et al. (2008) for example. In imbalanced sparse CCA, we need only to solve d Lasso optimization problems, which is fast, since d is small and Lasso can be efficiently solved by existing algorithms.

Second, because of this low dimensional structure, imbalanced sparse CCA can provide K pairs of canonical correlation vectors simultaneously, and does not need to obtain K pairs of canonical correlation vectors one by one. In particular, if one is only interested in the k-th pair of canonical vectors for k > 1, one does not need to know all l-th canonical vectors for l < k. Other methods mentioned above usually need to solve a separate optimization problem in order to get another pair of canonical vectors, and must know l-th pairs of canonical vectors for all l < k in order to get k-th pair of canonical vectors. This advantage of imbalanced sparse CCA makes our method extremely powerful when researchers need to estimate a relatively large number of pairs of canonical vectors.

Third, it is mentioned in Mai and Zhang (2019) that one advantage of their method is that they do not need any assumptions on the covariance matrices. In our algorithm, we only use the estimation of the covariance matrix at the last step. Therefore, our approach also does not require assumptions on the covariance matrices.

Fourth, because we solve d Lasso problems separately in imbalanced sparse CCA, our method naturally allows parallel computing, which can make our algorithm more efficient. The parallel computing makes imbalanced sparse CCA useful when p, n, and d are extremely large. This trivially parallel computing cannot be used by most methods mentioned above, where iteration is required.

Fifth, imbalanced sparse CCA has theoretical guarantees, and the theoretical development is much different from the other methods mentioned above. The theory underlying imbalanced sparse CCA involves not only statistical theory, but also results from numerical algebra. In our theoretical development, we are dealing with the eigenvalues and eigenvectors directly. Because we can obtain multiple eigenvectors at one time, we can obtain multiple canonical vectors simultaneously. Therefore, our theory and method may be able to inspire new directions of analysis and development of new methodologies for sparse CCA. Because of this new direction, our theory itself may be of interest to researchers studying sparse CCA.

4 Numeric Simulation

In this section, we conduct numeric studies on the applications of the imbalanced sparse CCA and sparse CCA methods. We compare the imbalanced sparse CCA (isCCA) with CCA with a nugget parameter (nCCA) as in (14) and (15), CCA with l_1 penalty (l_1 -CCA) (Witten et al., 2009), sCCA (Lee et al., 2011b), and regularized and sparse generalized CCA (rgCCA) (Tenenhaus and Tenenhaus, 2011). In our simulation study, we first simulate $X \sim N(0, \Sigma_{xx})$, $Y \sim N(0, \Sigma_{yy})$, with

$$\Sigma_{xx} = A_1 A_1^T + 0.1 I_p, \Sigma_{yy} = B_* \Sigma_{xx} B_*^T + \sigma^2 I_d, \Sigma_{xy} = \Sigma_{xx} B_*^T, \tag{17}$$

where $B_* \in \mathbb{R}^{d \times p}$ is a sparse matrix, $A_1 \in \mathbb{R}^{p \times d}$, $\sigma > 0$ is a parameter, and I_p and I_d are identity matrices with size p and d, respectively.

Given Σ_{xx} , B_* and σ^2 , we can calculate the k-th true canonical vectors by (4) and (5), denoted by a_k and b_k , respectively. In the numeric simulation, we mainly focus on the first pair of canonical vectors a_1 and b_1 . We use R packages PMA (Witten and Tibshirani, 2020), sCCA (Lee et al., 2011a), and RGCCA (Tenenhaus and Guillemot, 2017) to implement l_1 -CCA, sCCA, and rgCCA, respectively. For isCCA and nCCA, we generate an independent validation set of X_v and Y_v with the same sample size as the training set. The validation set is used to select the tuning parameters. Specifically, let $\lambda_1, ..., \lambda_m$ be candidates of tuning parameters, and $(\hat{a}'_{1,1}, \hat{b}'_{1,1}), ..., (\hat{a}'_{1,m}, \hat{b}'_{1,m})$ be the canonical vectors obtained by using parameters $\lambda_1, ..., \lambda_m$, respectively. Then we compute $\operatorname{corr}(Y_v^T a'_{1,j}, X_v^T b'_{1,j})$ for j = 1, ..., m, and choose $k = \operatorname{argmax}_{1 \le j \le m} \operatorname{corr}(Y_v^T a'_{1,j}, X_v^T b'_{1,j})$. The tuning parameter then is chosen to be λ_k , and the first pair of the estimated canonical vectors are $\hat{a}_1 = \hat{a}'_{1,k}$ and $\hat{b}_1 = \hat{b}'_{1,k}$. After obtaining estimated canonical vectors, we compare the l_2 errors $\|\hat{a}_1 - a_1\|_2$ and $\|\hat{b}_1 - b_1\|_2$ for all five methods.

Note in (17), the parameter σ^2 controls the correlation between x and y. Roughly speaking, a larger σ^2 leads to a smaller correlation between x and y. Therefore, we choose $\sigma^2 = 0.1k$, for k = 3, 4, ..., 30 to see the change of $\|\hat{a}_1 - a_1\|_2$ and $\|\hat{b}_1 - b_1\|_2$ when the correlation of x

and y changes. For each k, we run N = 50 replicates. For j-th replicate, we compute the estimated canonical vectors $\hat{a}_{1,j}$ and $\hat{b}_{1,j}$, and use

$$(\hat{\mathbb{E}}\|\hat{a} - a_1\|_2^2)^{1/2} = \sqrt{\frac{1}{N} \sum_{j=1}^N \|\hat{a}_{1,j} - a_1\|_2^2},$$
$$(\hat{\mathbb{E}}\|\hat{b} - b_1\|_2^2)^{1/2} = \sqrt{\frac{1}{N} \sum_{j=1}^N \|\hat{b}_{1,j} - b_1\|_2^2}$$

to approximate the root mean squared prediction error (RMSE)

$$(\mathbb{E}\|\hat{a} - a_1\|_2^2)^{1/2}, \quad (\mathbb{E}\|\hat{b} - b_1\|_2^2)^{1/2},$$

respectively. We consider two cases, where the matrix B_* is different. In both cases, we use the sample size n = 500. The matrix $A_1 = (\alpha_{jk})_{jk}$ is randomly generated by

$$\alpha_{jk}$$
 $\begin{cases} \sim \text{Unif}(0,2) & \text{with probability 0.3,} \\ = 0 & \text{with probability 0.7,} \end{cases}$

where Unif(0,2) is the uniform distribution on the interval [0,2].

Case 1:

In (17), we choose $B_* = (B_1, B_2)^T$, where

$$B_{1} = \begin{pmatrix} 2 & 1 & & & \\ 1 & 2 & 1 & & & \\ & 1 & \ddots & \ddots & \\ & & \ddots & \ddots & 1 \\ & & & 1 & 2 \end{pmatrix} \in \mathbb{R}^{d \times d}$$

is a tridiagonal matrix, and $B_2 \in \mathbb{R}^{d \times (p-d)}$ is a zero matrix. The results under different (p, d) are shown in Figures 1 - 3.

Case 2: We choose $B_* = (B_1, B_2)^T$ in (17), where

$$B_2 = \begin{pmatrix} & & & 1 & 2 \\ & & 1 & 2 & 1 \\ & 1 & \ddots & \ddots & \\ 1 & \ddots & \ddots & & \\ 2 & 1 & & & \end{pmatrix} \in \mathbb{R}^{d \times d},$$

and $B_1 \in \mathbb{R}^{d \times (p-d)}$ is a zero matrix. The results under different (p,d) are shown in Figures 4 - 6.

From Figures 1 - 6, we can see that sCCA performs well in most cases when estimating the first canonical vector a_1 . isCCA is comparable to rgCCA on the estimation of a_1 . l_1 -CCA cannot provide a consistent estimator of a_1 . nCCA does not perform well in Case 2. However,

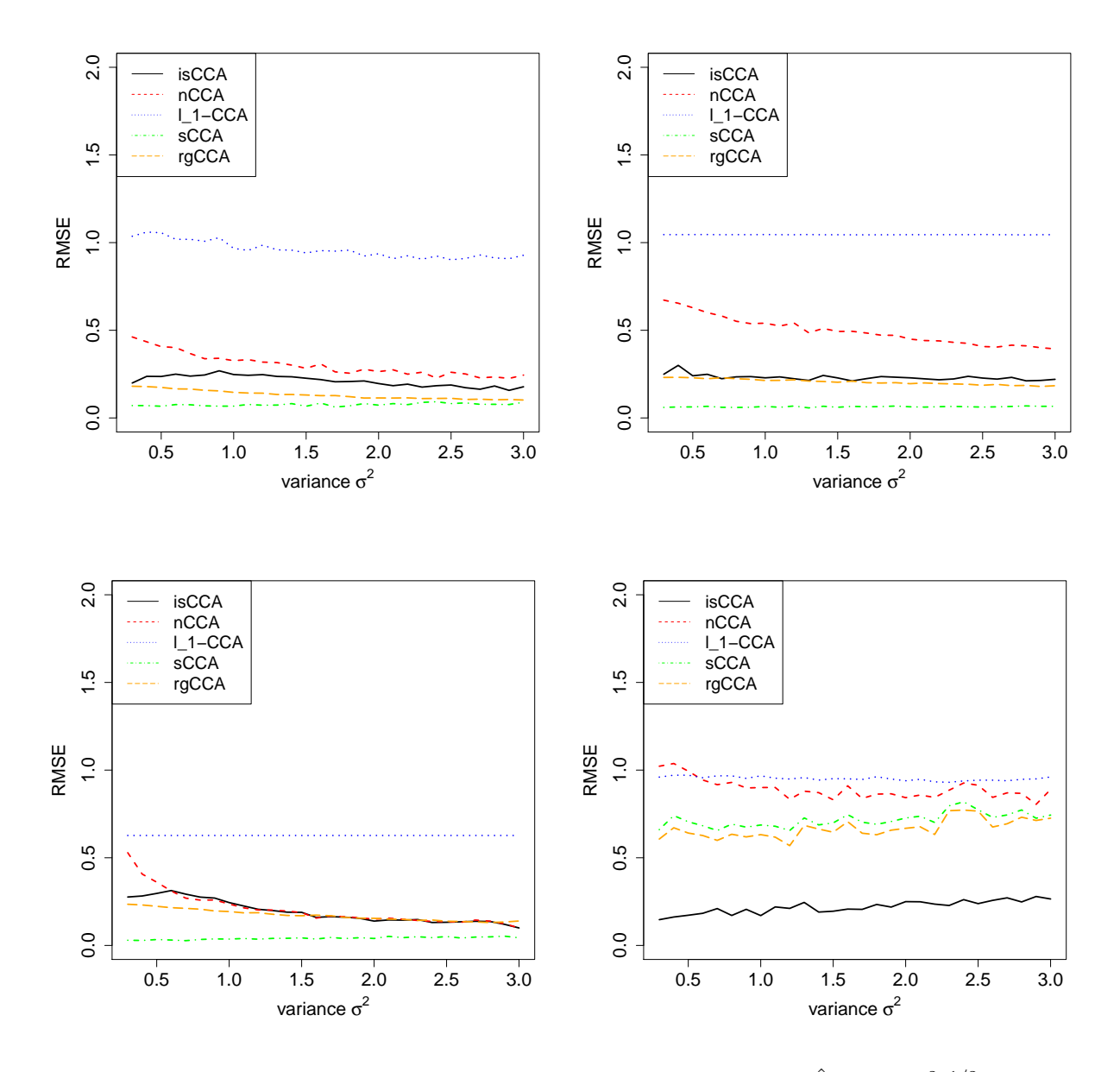


Figure 1: The approximated root mean squared prediction error $(\hat{\mathbb{E}} \| \hat{a} - a_1 \|_2^2)^{1/2}$ for Case 1. **Panel 1:** p = 100, d = 5. **Panel 2:** p = 100, d = 10. **Panel 3:** p = 500, d = 3. **Panel 4:** p = 1,000, d = 3.

when we turn to look at the estimation of the second canonical vector b_1 in the first pair of canonical vectors, we can see that nCCA, l_1 -CCA, sCCA, and rgCCA cannot provide a consistent estimator. Therefore, the average errors of these methods shown in Figure 3 and Figure 6 are large. This indicates that these methods are not appropriate when the dimensions of x and y are quite different, because these methods do not utilize the low dimensional structure of y. isCCA works well on the estimation of b_1 . We can also see the prediction error of isCCA increases as σ^2 increases, which is natural because the accuracy of the estimation of coefficients using (11) is influenced by the variance σ^2 .

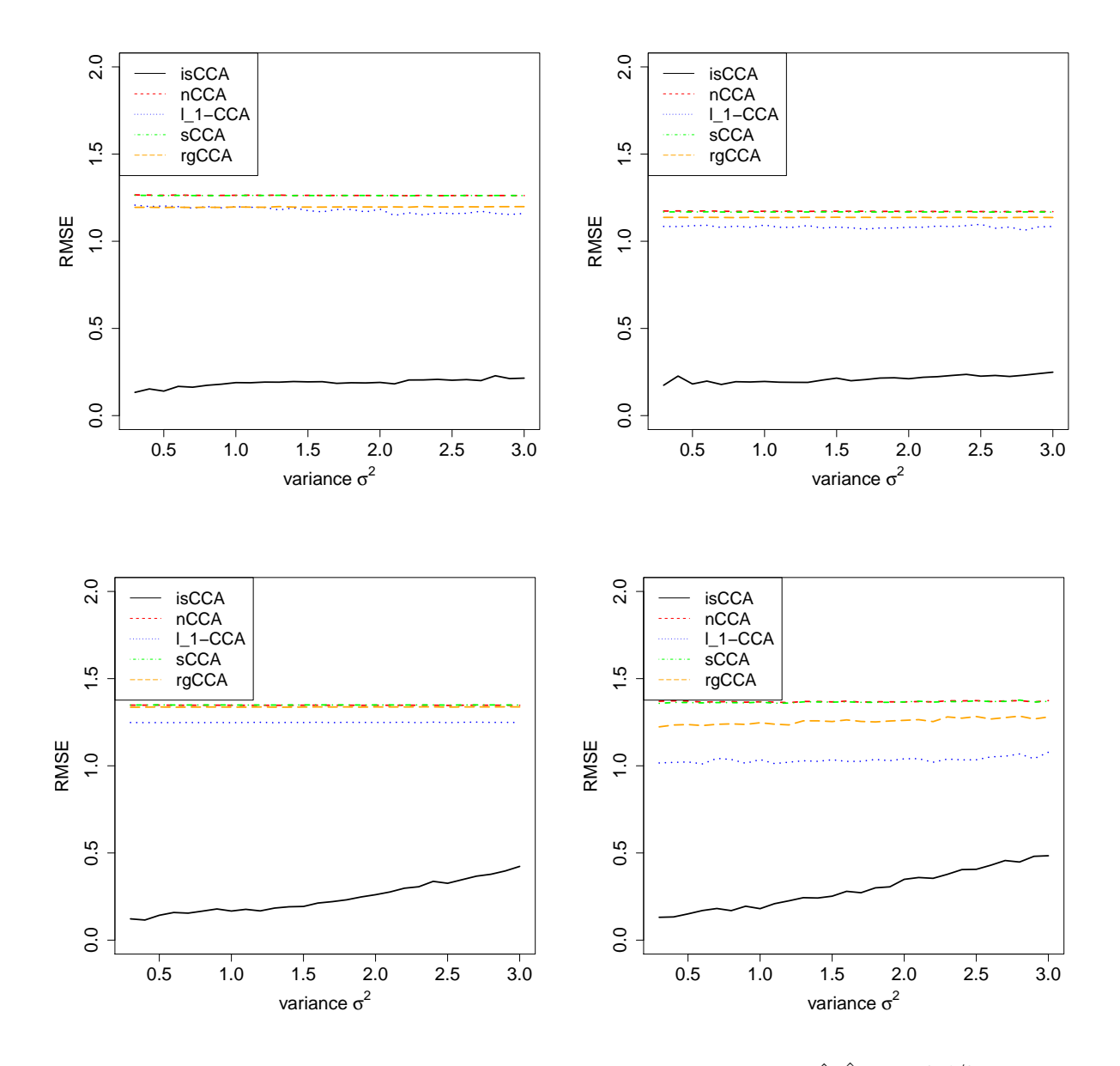


Figure 2: The approximated root mean squared prediction error $(\hat{\mathbb{E}}\|\hat{b} - b_1\|_2^2)^{1/2}$ for Case 1. **Panel 1:** p = 100, d = 5. **Panel 2:** p = 100, d = 10. **Panel 3:** p = 500, d = 3. **Panel 4:** p = 1,000, d = 3.

5 Real Data Examples

5.1 Analysis of Human Gut Microbiome Data

We applied imbalanced sparse CCA to a microbiome study conducted at University of Pennsylvania (Chen et al., 2012). The study profiled 16S rRNA in the human gut and measured components of nutrient intake using a food frequency questionnaire for 99 healthy people. Microbiome OTUs were consolidated at the genus level, with d=40 relatively

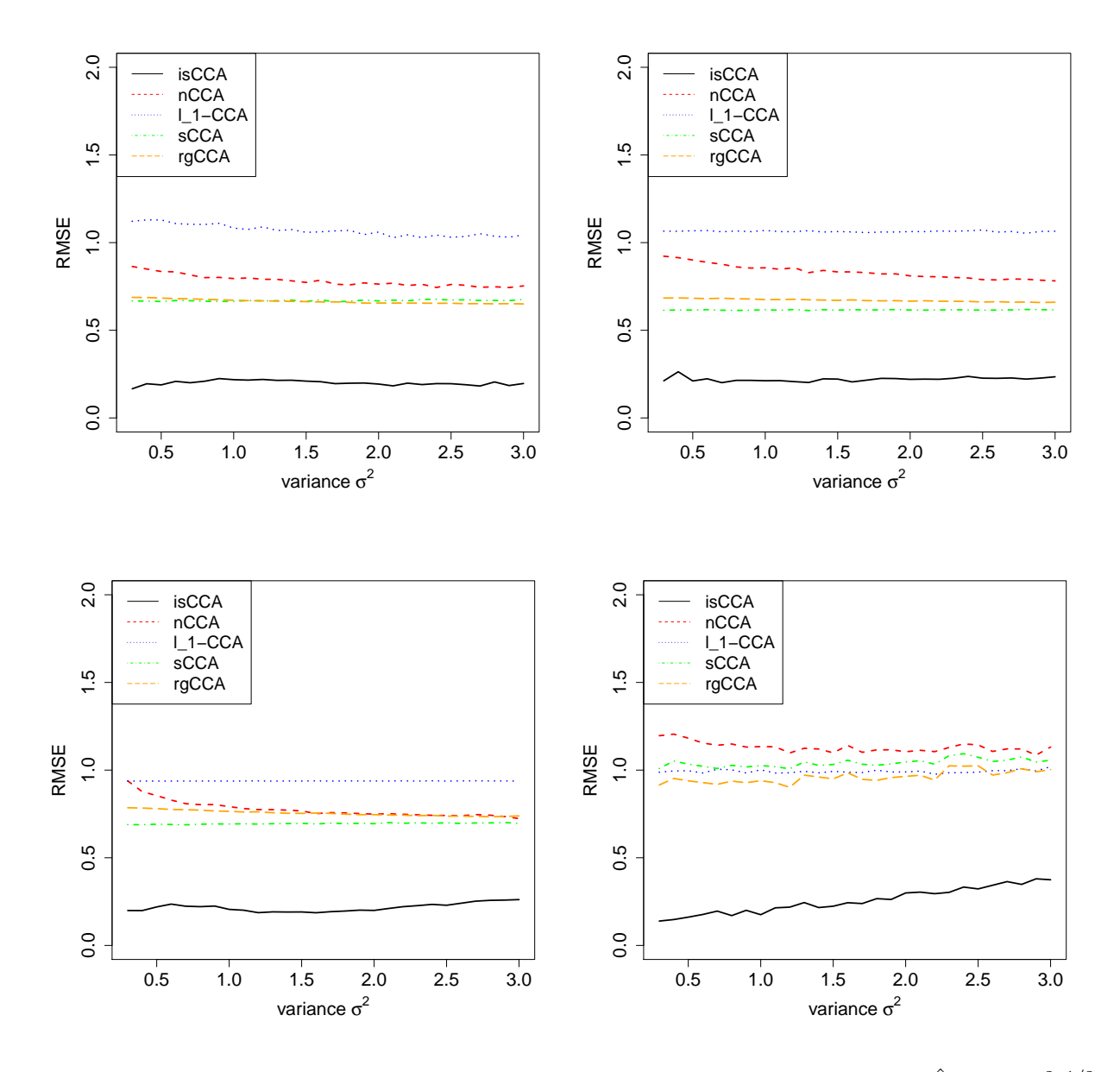


Figure 3: The average of approximated root mean squared prediction errors $(\hat{\mathbb{E}}\|\hat{a} - a_1\|_2^2)^{1/2} + (\hat{\mathbb{E}}\|\hat{b} - b_1\|_2^2)^{1/2})/2$ for Case 1. **Panel 1:** p = 100, d = 5. **Panel 2:** p = 100, d = 10. **Panel 3:** p = 500, d = 3. **Panel 4:** p = 1,000, d = 3.

common genera considered (i.e., Y was a 40×99 OTU abundance matrix). Following Chen et al. (2012), the daily intake for p=214 nutrients was calculated for each person, and regressed upon energy consumption, and the residuals used as a processed nutrient intake 214×99 matrix X.

ssCCA (Chen et al., 2012) identified 24 nutrients and 14 genera whose linear combinations gave a cross-validated canonical correlation of 0.42 between gut bacterial abundance and nutrients. Imbalanced sparse CCA reached a canonical correlation of 0.60. To test the canonical correlation between gut bacterial abundance and nutrients, we permuted columns of

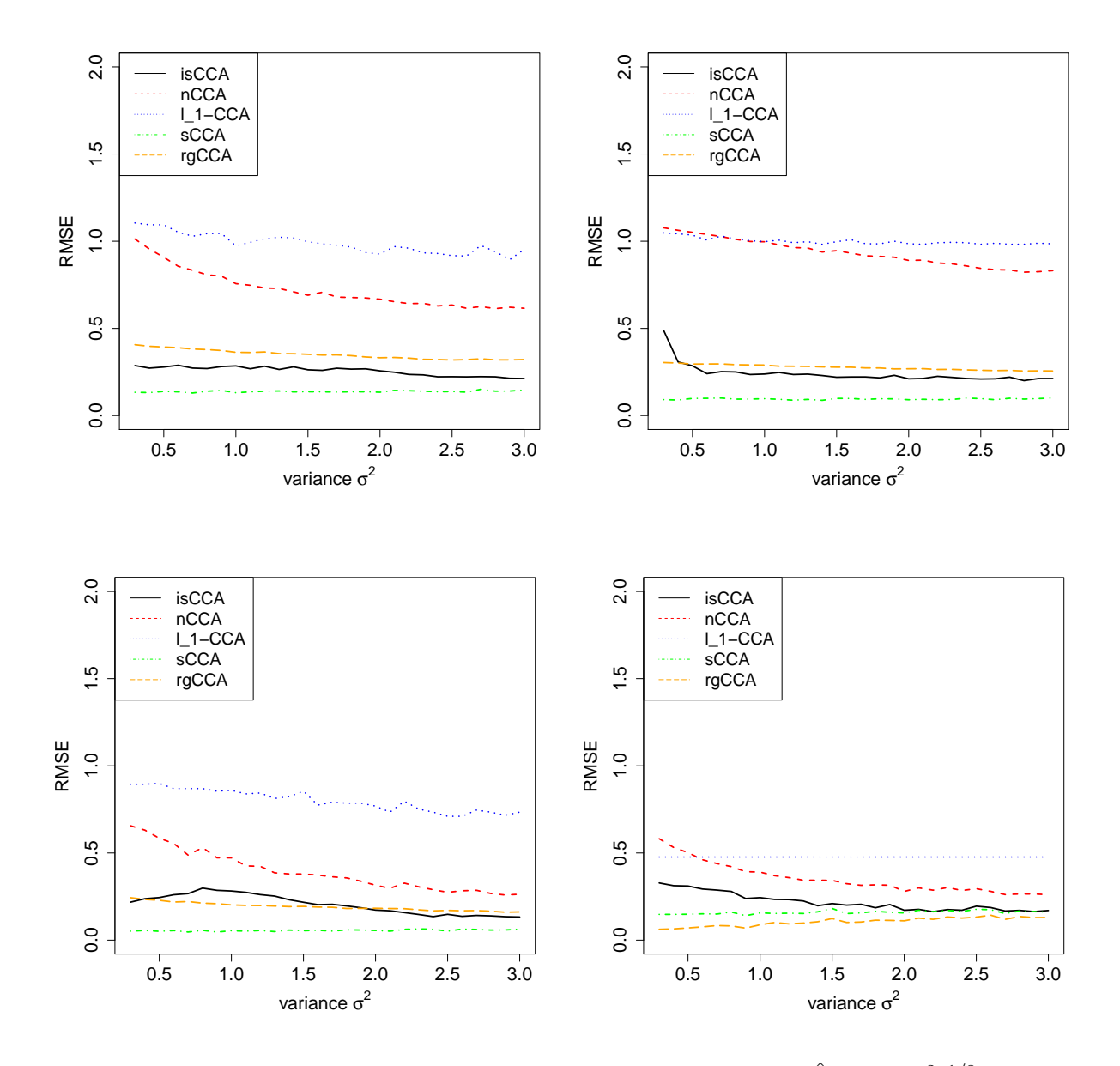


Figure 4: The approximated root mean squared prediction error $(\hat{\mathbb{E}} \| \hat{a} - a_1 \|_2^2)^{1/2}$ for Case 2. **Panel 1:** p = 100, d = 5. **Panel 2:** p = 100, d = 10. **Panel 3:** p = 500, d = 3. **Panel 4:** p = 1,000, d = 3.

the nutrient matrix 1,000 times, and calculated the canonical correlation between them using the five CCA methods described in Section 4. These correlations constitute a null distribution for each method, to which we compared the respective observed canonical correlation. The isCCA method was significant at the 0.05 level, with p-value 0.025. Of the remaining methods, only sCCA and nCCA (with a large nugget parameter) also provided significant p-values. However, results from nCCA appeared highly sensitive to the nugget parameter, and range of choices for nugget parameters produced nonsignificant p-values. l_1 -CCA and rgCCA did not appear to provide insightful results for this dataset. The heatmap of the covariance matrix

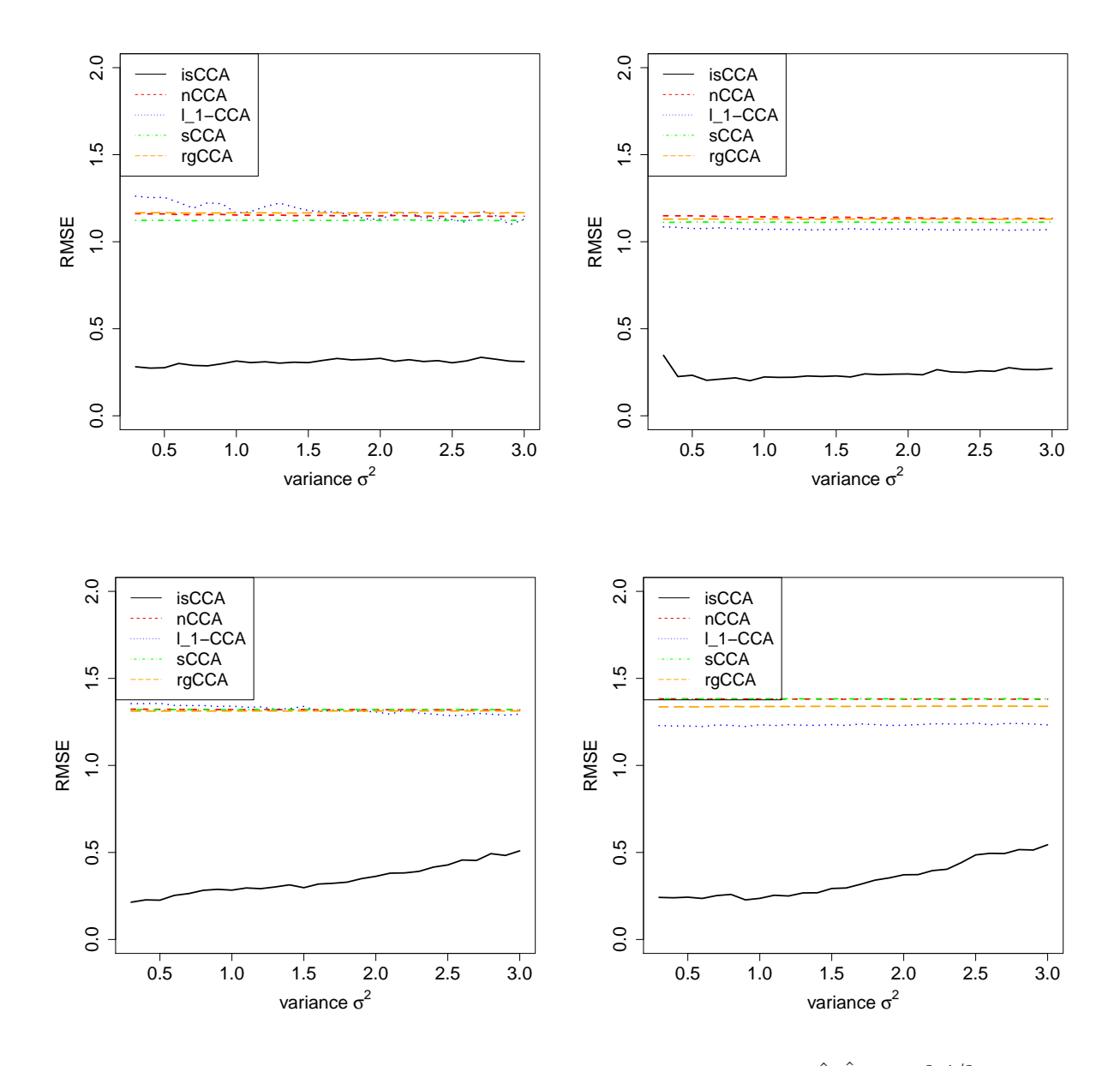


Figure 5: The approximated root mean squared prediction error $(\hat{\mathbb{E}} \| \hat{b} - b_1 \|_2^2)^{1/2}$ for Case 2. **Panel 1:** p = 100, d = 5. **Panel 2:** p = 100, d = 10. **Panel 3:** p = 500, d = 3. **Panel 4:** p = 1,000, d = 3.

 (XY^T) is shown in Figure 7. The marginal plots of absolute values of \hat{a}_1 and \hat{b}_1 provide insights for the relative weighting of OTUs and nutritional components toward the overall canonical correlation, i.e. larger values correspond to greater weight for that component.

5.2 Analysis of GTEx Thyroid Histology Images

The GTEx project offers an opportunity to explore the relationship between imaging and gene expression, while also considering the effect of a clinically-relevant trait. We obtained

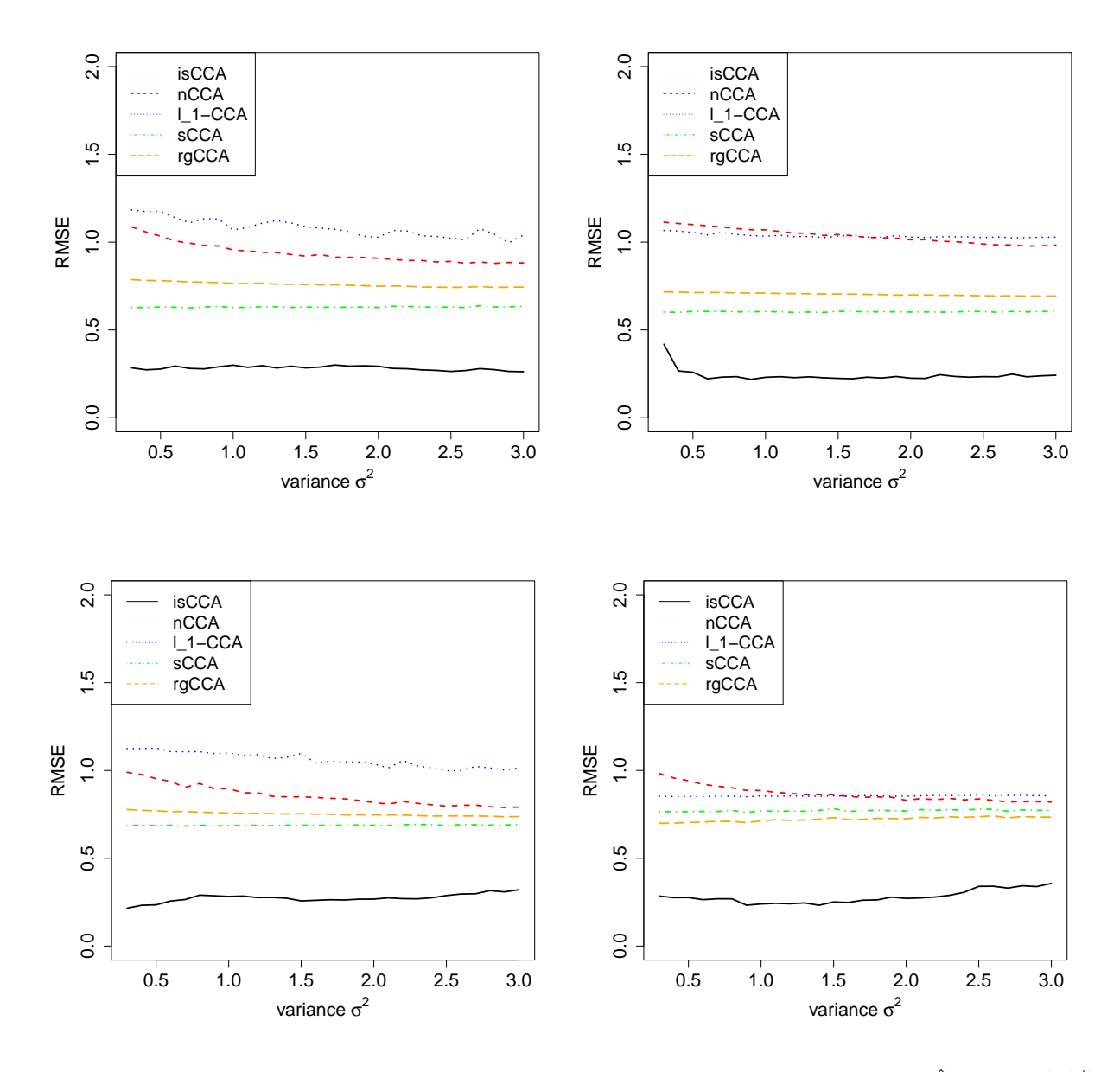


Figure 6: The average of approximated root mean squared prediction errors $(\hat{\mathbb{E}}\|\hat{a} - a_1\|_2^2)^{1/2} + (\mathbb{E}\|\hat{b} - b_1\|_2^2)^{1/2})/2$ for Case 2. **Panel 1:** p = 100, d = 5. **Panel 2:** p = 100, d = 10. **Panel 3:** p = 500, d = 3. **Panel 4:** p = 1,000, d = 3.

the original GTEx thyroid histology images (see Figure 8 for example) from the Biospecimen Research Database (https://brd.nci.nih.gov/brd/image-search/searchhome). These image files are in Aperio SVS format, a single-file pyramidal tiled TIFF. The RBioFormats R package (https://github.com/aoles/RBioFormats), which interfaces the OME Bio-Formats Java library (https://www.openmicroscopy.org/bio-formats), was used to convert the files to JPEG format. These images were further processed using the Bioconductor package EBImage (Pau et al., 2010). Following the method proposed by Barry et al. (2018) to segment individual tissue pieces, the average intensity across color channels was calculated, and adaptive thresholding

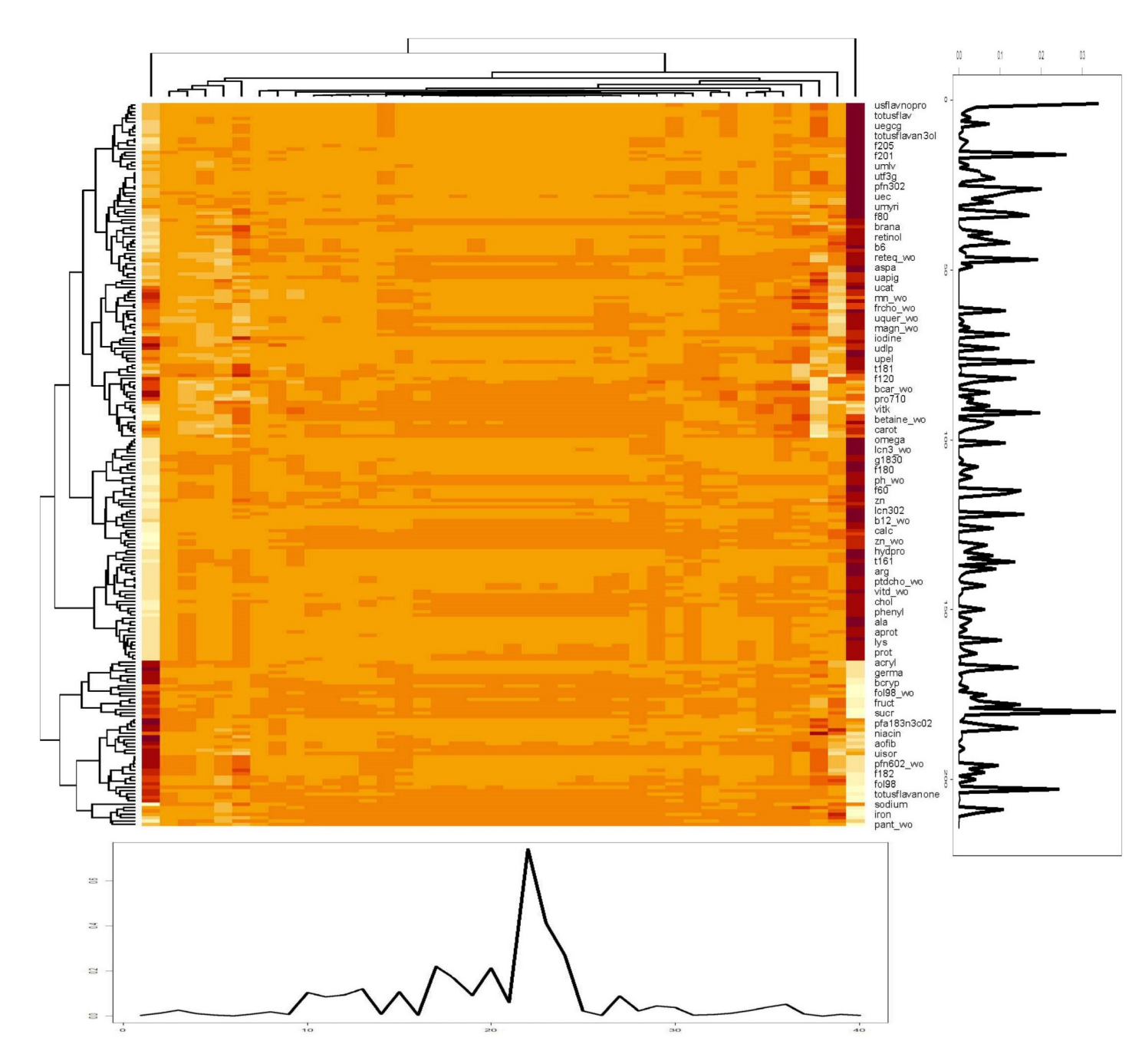


Figure 7: The heatmap of the covariance matrix between gut bacterial abundance and nutrients.

was performed to distinguish tissue from background. A total of 108 independent Haralick image features were extracted from each tissue piece by calculating 13 base Haralick features for each of the three RGB color channels and across three Haralick scales by sampling every 1, 10, or 100 pixels. The features were log2-transformed and normalized to ensure feature comparability across samples.

To obtain a trait with clinical relevance, we also downloaded the thyroiditis Hashimoto pathology data from the GTEx Portal (https://www.gtexportal.org/home/histologyPage).

Sex and age are also provided. The phenotype Hashimoto's thyroiditis was the presence (coded 1) or absence (0) of a particular pathology.

For thyroid, a subset of these subjects (570) also had gene expression data from RNA-Seq. The v8 release is available on the GTEx Portal (https://www.gtexportal.org/home/datasets). Gene read counts were normalized between samples using TMM, genes were selected based on expression thresholds explained in their paper (Aguet et al., 2019). In this example, we collect both processed image feature matrix (Y) and gene expression data (X) on these overlapped 570 subjects, with 37 cases of Hashimoto's thyroiditis.

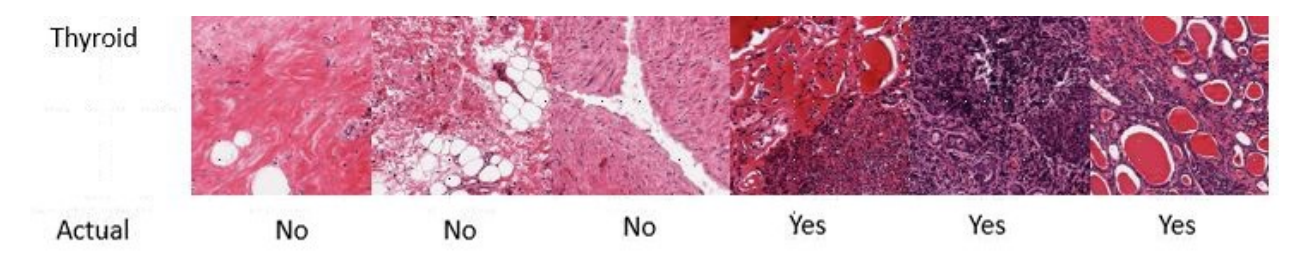


Figure 8: Examples of Hashimoto's thyroiditis negative/positive GTEx samples.

We applied imbalanced sparse CCA and other four methods in Section 4, to study the correlation between the processed image feature matrix and gene expression data. Since imbalanced sparse CCA works well for the low dimensional data Y, we first applied principal component analysis (PCA) to reduce the dimension of Y. We used the first half of principal components, denoted by $U = (u_1, ..., u_d)$, and performed imbalanced sparse canonical correlation analysis on the transformed variables UY and X. We randomly split the data into a training set (Y^{train}, X^{train}) and testing set (Y^{test}, X^{test}) with ratio 5:1 for 500 times. For each run, we obtained the first pair of estimated canonical vectors \hat{a}_1 and \hat{b}_1 by the methods mentioned in Section 4, and compared the correlations on the testing set $\text{corr}((Y^{test})^T\hat{a}_1, (X^{test})^T\hat{b}_1)$. We found that nCCA is very sensitive to the value of the nugget parameter, so we did not include it in the comparison. The results obtained by isCCA, l_1 -CCA, sCCA and rgCCA are shown in Figure 9.

From Figure 9, we can see that rgCCA does not provide reliable estimation of the canonical variables in this study, and sCCA provides a smaller correlation between the estimated canonical variables on the testing data. isCCA is slightly better than l_1 -CCA. In some cases, isCCA provides relatively small correlations between the estimated canonical variables on the testing data. This may be because we fixed the number of principal components. Therefore, a further study on adaptively choosing number of principal components is needed.

In order to explore the effect of a clinical phenotype on isCCA, we performed isCCA separately on the set of individuals without Hashimoto's thyroiditis (median isCCA of 0.578, nearly the same as for the full dataset), and for individuals with Hashimoto's thyroiditis (median isCCA of 0.375). The dramatic change in estimated correlation by case/control status provides a window into potential additional uses of sparse CCA methods, e.g. by using the contrast in canonical correlation by phenotype to improve omics-based phenotype prediction.

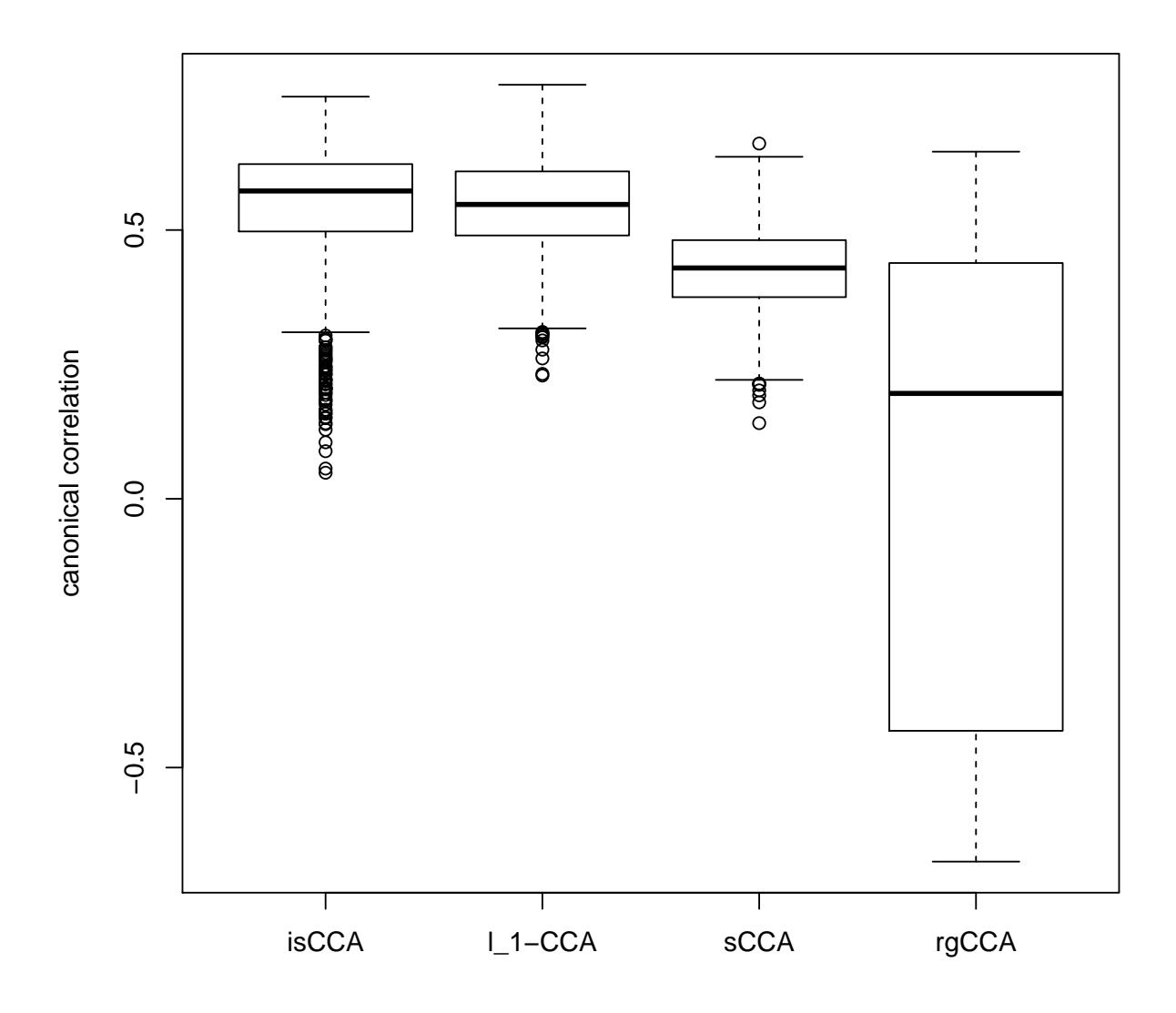


Figure 9: Boxplots of the GTEx thyroid cross-validated canonical correlations of processed image feature matrix and gene expression data.

5.3 Analysis of SNP Genotype Data and RNA-seq Gene Expression Data

We tested imbalanced sparse CCA and other four methods in Section 4 using data from the GTEx V8 release (https://www.gtexportal.org/home/), including genotype data from a selected set of SNPs and RNA-seq gene expression data from n=208 liver tissue samples. SNPs were coded from 0-2 as the number of minor alleles, and RNA-seq expression data were normalized using simple scaling. Among the problems that arise in such datasets is

the powerful mapping of sets of SNPs that are collectively associated with expression traits. Here we use CCA to demonstrate a proof of principle for finding such collective association in a biological pathway. We selected SNP sets for each gene by grouping SNPs located within 5kb of a gene's transcription start site (TSS). Then we grouped genes into gene sets based on the canonical pathways listed in the Molecular Signatures Database (MSigDB) v7.0 (https://www.gsea-msigdb.org/gsea/msigdb/index.jsp). These gene sets are canonical representations of a biological process compiled by domain experts. We analyzed 2,072 pathways with a size between 5-200 genes. So for each pathway, we have a genotype matrix X with p SNPs and p samples and expression matrix p with p genes and p samples, with p samples are calculated after performing 1,000 permutations.

Here we focus on two pathways of potential biological relevance in the liver, with strong eQTL evidence. One is the keratinization pathway (https://www.reactome.org/content/detail/R-HSA-6805567), which included 72 genes and 3,005 SNPs from our dataset. The p-values were 0.006, 0.10, 0.68, 0.14, and 0.81 for isCCA, nCCA, sCCA, l_1 -CCA, and rgCCA respectively. Three genes, KRT13, KRT4, and KRT5, showed values of $|\hat{a}|$ that are much larger than those of the remaining genes, while the values of \hat{b} are spread more uniformly across the SNPs. Keratins are important for the mechanical stability and integrity of epithelial cells and liver tissues. They play a role in protecting liver cells from apoptosis, against stress, and from injury, and defects may predispose to liver diseases (Moll et al., 2008). Figure 10 shows heatmap plots and Manhattan-style line plots showing the absolute values of \hat{a} and \hat{b} , in which SNPs (rows) and genes (columns) are ordered by genomic position.

A smaller pathway is the synthesis of ketone bodies (https://www.reactome.org/content/detail/R-HSA-77111), with 8 genes and 265 SNPs. The p-values were 0.003, 0.16, 0.52, 0.35, and 0.66 for isCCA, nCCA, sCCA, l_1 -CCA, and rgCCA respectively. Again three genes, ACSS3, BDH2, and BDH1 showed $|\hat{a}|$ of greater magnitude than the others. Ketone bodies are metabolites derived from fatty and amino acids and are mainly produced in the liver. Both in the biosynthesis of ketone bodies (ketogenesis) and in ketone body utilization (ketolysis), inborn errors of metabolism are known, resulting in various metabolic diseases (Sass, 2012).

6 Conclusions and Discussion

In this work, we proposed imbalanced sparse canonical correlation analysis, which can be applied to data where the dimensions of two variables are very different. Our method can provide K pairs of canonical vectors simultaneously for K > 1, and can be implemented by an efficient algorithm based on Lasso. The implementation is straightforward. The computation time can be significantly decreased if parallel computing is available. We show the consistency of the estimated canonical pairs in the case that the dimension of one variable can increase as an exponential rate in comparison to the sample size. The dimension of the other variable should be smaller than the sample size. We also present numerical studies and real data analysis to validate our methodology.

We consider the *imbalanced* case, where the dimensions of two variables are much different. In practice, there are also some cases that are *balanced*, i.e., the dimensions of two variables are comparable but both much larger than the sample size. One straightforward potential

extension is to apply two sets of Lasso problems. Specifically, we might set Y as the dependent variable and X as the independent variable in the first set of Lasso problems, and set X as the dependent variable and Y as the independent variable in the second set of Lasso problems. However, the number of Lasso optimizations is very large, which leads to the inefficiency of the algorithm. One possible remedy is to apply principal components analysis to reduce the dimension of one variable. This approach has shown its potential in the real data analysis. However, the theoretical justification is currently lacking. Imbalanced sparse canonical correlation analysis also shows great potential for prediction problems, since it can provides K pairs of canonical vectors simultaneously for K > 1. These possible extensions of imbalanced sparse canonical correlation analysis to the balanced case will be pursued in the future work.

Appendix

A Notation

We first present some notation used in Appendix. Let $A = (a_{ij})_{ij} \in \mathbb{R}^{m \times n}$. Let $||A||_p$ be the p-norm of a matrix A, defined by

$$||A||_p = \sup_{x \neq 0} \frac{||Ax||_p}{||x||_p},$$

where $||x||_p$ is the l_p norm of a vector $x \in \mathbb{R}^n$. With an abuse of notation, we use $||\cdot||_p$ for both p-norm of a matrix and l_p norm of a vector. Let $||A||_{\max} = \max |a_{ij}|$. In the special cases $p = 1, 2, \infty$,

$$||A||_1 = \max_{1 \le j \le n} \sum_{i=1}^m |a_{ij}|, \quad ||A||_2 = \sigma_{\max}(A), \quad ||A||_{\infty} = \max_{1 \le i \le m} \sum_{j=1}^n |a_{ij}|,$$

where $\sigma_{\text{max}}(A)$ is the largest singular value of matrix A. These matrix norms are equivalent, which are implied by the following inequality,

$$\frac{1}{\sqrt{n}} \|A\|_{\infty} \le \|A\|_{2} \le \sqrt{m} \|A\|_{\infty},$$

$$\frac{1}{\sqrt{m}} \|A\|_{1} \le \|A\|_{2} \le \sqrt{n} \|A\|_{1},$$

$$\|A\|_{\max} \le \|A\|_{2} \le \sqrt{mn} \|A\|_{\max}.$$

B Proof of Proposition 1

Recall in (8), we have

$$\Sigma_{yy} = B_* \Sigma_{xx} B_*^T + \Sigma_{\epsilon_y \epsilon_y}.$$

By Weyl's theorem (Horn and Johnson (2012), Theorem 4.3.1), we have

$$\lambda_{\min}(\Sigma_{yy}) \ge \lambda_{\min}(\Sigma_{\epsilon_y \epsilon_y}) + \lambda_{\min}(B_* \Sigma_{xx} B_*^T) \ge \lambda_{\min}(\Sigma_{\epsilon_y \epsilon_y}) \ge K_1,$$

where the last inequality is because of Assumption 1. Using Weyl's theorem again, we can bound the largest eigenvalue $\lambda_{\max}(\Sigma_{yy})$ by

$$\lambda_{\max}(\Sigma_{yy}) \leq \lambda_{\max}(\Sigma_{\epsilon_y \epsilon_y}) + \lambda_{\max}(B_* \Sigma_{XX} B_*^T)$$

$$\leq \lambda_{\max}(\Sigma_{\epsilon_y \epsilon_y}) + \|B_*\|_2^2 \lambda_{\max}(\Sigma_{XX}) \leq K_2,$$

where the last inequality is because of Assumptions 1 and 2. This finishes the proof.

C Proof of Theorem 1

We first present some lemmas used in this proof. Lemma C.1 states the consistency of $\hat{\beta}_k$ obtained by (12). Lemma C.2 is the Bernstein inequality. Lemma C.3 is the concentration inequality for sub-Gaussian random vectors. Lemma C.4 describes the accuracy of solving linear systems; see Theorem 2.7.3 in Van Loan and Golub (1983). Lemma C.5 states the eigenvector sensitivity for a pertubation of a matrix, which is a slight recasting of Theorem 4.11 in Stewart (1973); also see Corollary 7.2.6 in Van Loan and Golub (1983).

Lemma C.1. Suppose the conditions of Theorem 1 hold. Then with probability at least $1 - C_1 p^{-1} d$,

$$\max_{1 \le k \le d} \|\hat{\beta}_k - \beta_k^*\|_1 \le C_2 s^* \sqrt{\frac{\log p}{n}}, \max_{1 \le k \le d} \|\hat{\beta}_k - \beta_k^*\|_2 \le C_3 \sqrt{\frac{s^* \log p}{n}}.$$

In addition, $\max_{1 \le k \le d} (\hat{\beta}_k - \beta_k^*)^T H_X(\hat{\beta}_k - \beta_k^*) \lesssim s^* \log p/n$, where $H_X = n^{-1} \sum_{i=1}^n X_i X_i^T$.

Proof. By Lemma B.3 of Ning and Liu (2017), we have for a fixed k, with probability at least $1 - C_1 p^{-1}$,

$$\|\hat{\beta}_k - \beta_k^*\|_1 \le C_2 s^* \sqrt{\frac{\log p}{n}}, \|\hat{\beta}_k - \beta_k^*\|_2 \le C_3 \sqrt{\frac{s^* \log p}{n}}, (\hat{\beta}_k - \beta_k^*)^T H_X(\hat{\beta}_k - \beta_k^*) \lesssim \frac{s^* \log p}{n}.$$

Then the results follow the union bound inequality.

Lemma C.2. Let X_i 's be independent mean zero sub-Gaussian variables. There exists a constant C > 0 such that for any t > 0,

$$\mathbb{P}\left(\frac{1}{n}\left|\sum_{i=1}^{n} X_i\right| \ge t\right) \le 2\exp(-Cnt^2).$$

Lemma C.3. Let $Q_i \in \mathbb{R}^d$ be sub-Gaussian random vectors for i = 1, ..., n. We have

$$\mathbb{P}(\|H_Q - \mathbb{E}(QQ^T)\|_{\max} \ge t) \le 2q^2 \exp(-C_1 nt^2),$$

for some constants $C_1, C_2 > 0$, where $H_Q = n^{-1} \sum_{i=1}^n Q_i Q_i^T$.

Proof. The results follow the union bound inequality and Lemma C.2.

Lemma C.4. Let $A, \tilde{A} \in \mathbb{R}^{d \times d}$, and $b, \tilde{b} \in \mathbb{R}^d$. Suppose Ax = b and $\tilde{A}\tilde{x} = \tilde{b}$ with $\|\tilde{A} - A\|_2 \le \delta \|A\|_2$, $\|\tilde{b} - b\|_2 \le \delta \|b\|_2$, and $\kappa(A) = r/\delta < 1/\delta$ for some $\delta > 0$. Then, \tilde{A} is non-singular,

П

$$\frac{\|\tilde{x}\|_{2}}{\|x\|_{2}} \le \frac{1+r}{1-r},$$

$$\frac{\|\tilde{x}-x\|_{2}}{\|x\|_{2}} \le \frac{2\delta}{1-r}\kappa(A),$$

where $\kappa(A) = ||A||_2 ||A^{-1}||_2$.

Lemma C.5. Let $A, E \in \mathbb{R}^{d \times d}$ and $Q = [q_1, Q_2] \in \mathbb{R}^{d \times d}$ is orthogonal, where $q_1 \in \mathbb{R}^d$. Let

$$Q^{T}AQ = \begin{bmatrix} \lambda & v^{T} \\ 0 & T_{22} \end{bmatrix}, Q^{T}EQ = \begin{bmatrix} \epsilon & r^{T} \\ \delta & E_{22} \end{bmatrix}.$$

If $\sigma = \sigma_{\min}(T_{22} - \lambda I) > 0$ and

$$||E||_2 \left(1 + \frac{5||v||_2}{\sigma}\right) \le \frac{\sigma}{5},$$

then there exists $u \in \mathbb{R}^{d-1}$ with

$$||u||_2 \leq 4 \frac{||\delta||_2}{\sigma}$$

such that $\tilde{q}_1 = (q_1 + Q_2 u)/\sqrt{1 + u^T u}$ is a unit 2-norm eigenvector for A + E.

Now we are ready to prove Theorem 1. We first show that $(YY^T)^{-1}\hat{B}X(\hat{B}X)^T$ is close to $\Sigma_{yy}^{-1}B_*\Sigma_{xx}B_*^T$, then we apply Lemma C.5 to show the consistency of canonical vectors. Without loss of generality, let k=1. If (13) holds for k=1, then the results of Theorem 1 follow the union bound inequality.

By the triangle inequality, the 2-norm of $(YY^T)^{-1}\hat{B}X(\hat{B}X)^T - \Sigma_{yy}^{-1}B_*\Sigma_{xx}B_*^T$ can be bounded by

$$\| (YY^{T})^{-1} \hat{B}X(\hat{B}X)^{T} - \Sigma_{yy}^{-1} B_{*} \Sigma_{xx} B_{*}^{T} \|_{2}$$

$$\leq \left\| (\frac{1}{n} YY^{T})^{-1} \frac{1}{n} \hat{B}X(\hat{B}X)^{T} - \Sigma_{yy}^{-1} \frac{1}{n} \hat{B}X(\hat{B}X)^{T} + \Sigma_{yy}^{-1} \frac{1}{n} \hat{B}X(\hat{B}X)^{T} - \Sigma_{yy}^{-1} \frac{1}{n} B_{*}X(B_{*}X)^{T} \right.$$

$$+ \left. \Sigma_{yy}^{-1} \frac{1}{n} B_{*}X(B_{*}X)^{T} - \Sigma_{yy}^{-1} B_{*} \Sigma_{xx} B_{*}^{T} \right\|_{2}$$

$$\leq \left\| (\frac{1}{n} YY^{T})^{-1} \frac{1}{n} \hat{B}X(\hat{B}X)^{T} - \Sigma_{yy}^{-1} \frac{1}{n} \hat{B}X(\hat{B}X)^{T} \right\|_{2} + \left\| \Sigma_{yy}^{-1} \frac{1}{n} \hat{B}X(\hat{B}X)^{T} - \Sigma_{yy}^{-1} \frac{1}{n} B_{*}X(B_{*}X)^{T} \right\|_{2}$$

$$+ \left\| \Sigma_{yy}^{-1} \frac{1}{n} B_{*}X(B_{*}X)^{T} - \Sigma_{yy}^{-1} B_{*} \Sigma_{xx} B_{*}^{T} \right\|_{2}$$

$$= I_{1} + I_{2} + I_{3}.$$

$$(C.1)$$

We consider I_2 first. By Assumption 1, we have

$$\begin{split} I_{2} &\leq \left\| \Sigma_{yy}^{-1} \right\|_{2} \left\| \frac{1}{n} \hat{B} X (\hat{B} X)^{T} - \frac{1}{n} B_{*} X (B_{*} X)^{T} \right\|_{2} \\ &\leq \frac{1}{K_{1}} \|B_{*} H_{X} B_{*}^{T} - \hat{B} H_{X} B_{*}^{T} + \hat{B} H_{X} B_{*}^{T} - \hat{B} H_{X} \hat{B}^{T} \|_{2} \\ &= \frac{1}{K_{1}} \| (B_{*} - \hat{B}) H_{X} (B_{*} + \hat{B})^{T} \|_{2} \\ &\leq \frac{1}{K_{1}} \sqrt{\| (B_{*} - \hat{B}) H_{X} (B_{*} - \hat{B})^{T} \|_{2} \| (B_{*} + \hat{B}) H_{X} (B_{*} + \hat{B})^{T} \|_{2}}, \end{split}$$
 (C.2)

where $H_X = \frac{1}{n} \sum_{i=1}^n X_i X_i^T$, and the third inequality is because of the Cauchy-Schwarz inequality.

The first term in the right-hand side of (C.2) $||(B_* - \hat{B})H_X(B_* - \hat{B})^T||_2$ can be bounded by

$$||(B_* - \hat{B})H_X(B_* - \hat{B})^T||_2 \le \operatorname{tr}((B_* - \hat{B})H_X(B_* - \hat{B})^T)$$

$$\le d \max_k (\hat{\beta}_k - \beta_k^*)^T H_X(\hat{\beta}_k - \beta_k^*)$$

$$\lesssim ds^* \log p/n, \tag{C.3}$$

where tr(A) is the trace of a matrix A, and the last inequality is by Lemma C.1. The second term in (C.2) $(B_* + \hat{B})H_X(B_* + \hat{B})^T$ can be bounded by

$$||(B_* + \hat{B})H_X(B_* + \hat{B})^T||_2 = ||(\hat{B} - B_* + 2B_*)H_X(\hat{B} - B_* + 2B_*)^T||_2$$

$$\leq 2||(\hat{B} - B_*)H_X(B_* - \hat{B})^T + 4B_*H_XB_*^T||_2$$

$$\leq 2||(\hat{B} - B_*)H_X(B_* - \hat{B})^T||_2 + 8||B_*H_XB_*^T||_2$$

$$\lesssim ds^* \log p/n + ||B_*H_XB_*^T||_2, \qquad (C.4)$$

where the first inequality is by the Cauchy-Schwarz inequality, the second inequality is by the triangle inequality, and the third inequality is by (C.3).

Now consider bounding $||B_*H_XB_*^T||_2$. By the triangle inequality, we have $||B_*H_XB_*^T||_2 \le ||B_*\Sigma_{xx}B_*^T||_2 + ||B_*\Sigma_{xx}B_*^T - B_*H_XB_*^T||_2$. Therefore, we need to show that $||B_*\Sigma_{xx}B_*^T - B_*H_XB_*^T||_2$ is small, which can be shown directly by Lemma C.3. To see this, note that B_*X_i is still a sub-Gaussian random vector. Let $t = C_2\sqrt{\log(d+p)/n}$ for some constant $C_2 > 0$ in Lemma C.3. By Lemma C.3, with probability at least $1 - d^2/p$, we have

$$||B_*\Sigma_{xx}B_*^T - B_*H_XB_*^T||_{\max} \lesssim \sqrt{\frac{\log(d+p)}{n}},$$

which implies

$$||B_* \Sigma_{xx} B_*^T - B_* H_X B_*^T||_2 \le d||B_* \Sigma_{xx} B_*^T - B_* H_X B_*^T||_{\max} \lesssim d\sqrt{\frac{\log(d+p)}{n}}.$$
 (C.5)

By Assumption 1, Proposition 1 and (8), we have

$$||B_*\Sigma_{xx}B_*^T||_2 = ||\Sigma_{yy} - \Sigma_{\epsilon_y \epsilon_y}||_2 \le ||\Sigma_{yy}||_2 + ||\Sigma_{\epsilon_y \epsilon_y}||_2 \le C_3,$$

for some constant $C_3 > 0$. Therefore, with probability at least $1 - d^2/p$, the right hand side of (C.4) can be further bounded by

$$\|(B_* + \hat{B})H_X(B_* + \hat{B})^T\|_2 \lesssim ds^* \log p/n + d\sqrt{\frac{\log(d+p)}{n}} + C_3.$$
 (C.6)

Plugging (C.3) and (C.6) into (C.2), we have

$$I_2 \lesssim \sqrt{ds^* \log p/n}.$$
 (C.7)

The first term I_1 in (C.1) can be bounded by

$$I_1 \le \left\| \left(\frac{1}{n} Y Y^T \right)^{-1} - \Sigma_{yy}^{-1} \right\|_2 \left\| \frac{1}{n} \hat{B} X (\hat{B} X)^T \right\|_2.$$
 (C.8)

By letting $t = C_4 \sqrt{\log(d+p)/n}$ for some constant $C_4 > 0$ in Lemma C.3, with probability at least $1 - d^2/p$, we have

$$\left\| \frac{1}{n} Y Y^T - \Sigma_{yy} \right\|_2 \le d \left\| \frac{1}{n} Y Y^T - \Sigma_{yy} \right\|_{\text{max}} \lesssim d \sqrt{\log(d+p)/n}.$$

For any unit vector u, by Lemma C.4 and noting that Proposition 1 implies $\kappa(\Sigma_{yy}) \leq C_5$, we have

$$\left\| \left(\frac{1}{n} Y Y^T \right)^{-1} u - \Sigma_{yy}^{-1} u \right\|_2 \lesssim d \sqrt{\log(d+p)/n},$$

which implies

$$\left\| \left(\frac{1}{n} Y Y^T \right)^{-1} - \Sigma_{yy}^{-1} \right\|_2 \lesssim d\sqrt{\log(d+p)/n}. \tag{C.9}$$

The second term in the right-hand side of (C.8) can be bounded by

$$\begin{aligned} \left\| \frac{1}{n} \hat{B} X (\hat{B} X)^T \right\|_2 &= \left\| \frac{1}{n} \hat{B} X (\hat{B} X)^T - \frac{1}{n} B_* X (B_* X)^T + \frac{1}{n} B_* X (B_* X)^T \right\|_2 \\ &\leq \left\| \frac{1}{n} \hat{B} X (\hat{B} X)^T - \frac{1}{n} B_* X (B_* X)^T \right\|_2 + \left\| \frac{1}{n} B_* X (B_* X)^T \right\|_2, \end{aligned}$$

which can be bounded by a constant using the similar approach as in bounding I_2 . Together with (C.8) and (C.9), we have

$$I_1 \lesssim d\sqrt{\log(d+p)/n}.$$
 (C.10)

By Proposition 1 and (C.5), it can be verified that the term I_3 can be bounded by

$$I_{3} = \left\| \Sigma_{yy}^{-1} \frac{1}{n} B_{*} X (B_{*} X)^{T} - \Sigma_{yy}^{-1} B_{*} \Sigma_{xx} B_{*}^{T} \right\|_{2}$$

$$\leq \left\| \Sigma_{yy}^{-1} \right\|_{2} \left\| \frac{1}{n} B_{*} X (B_{*} X)^{T} - B_{*} \Sigma_{xx} B_{*}^{T} \right\|_{2}$$

$$\lesssim d \sqrt{\log(d+p)/n}. \tag{C.11}$$

Plugging (C.7), (C.10) and (C.11) in (C.1), we have

$$\|(YY^{T})^{-1}\hat{B}X(\hat{B}X)^{T} - \Sigma_{yy}^{-1}B_{*}\Sigma_{xx}B_{*}^{T}\|_{2} \lesssim d\sqrt{\log(d+p)/n} + \sqrt{ds^{*}\log p/n}$$

$$\lesssim d\sqrt{\log p/n} + \sqrt{ds^{*}\log p/n},$$
(C.12)

where the last inequality is because d < p.

To apply Lemma C.5, we need to show that $\|\delta\|_2$ in Lemma C.5 is small. Let $E = (YY^T)^{-1}\hat{B}X(\hat{B}X)^T - \sum_{uu}^{-1}B_*\sum_{xx}B_*^T$. By (C.12), we have

$$\|\delta\|_2 = \|Q_2^T E q_1\|_2 \le \|Q_2^T E\|_2 \le \|Q_2\|_2 \|E\|_2 \lesssim \sqrt{d^2 \log p/n} + \sqrt{ds^* \log p/n} \lesssim \sqrt{d(d+s^*) \log p/n},$$

where Q is as in Assumption 3, and the last inequality follows the fact $\sqrt{w_1} + \sqrt{w_2} \le \sqrt{2w_1 + 2w_2}$ for $w_1, w_2 > 0$. By Assumption 3, we can apply Lemma C.5. This yields

$$||a_1 - \hat{a}_1||_2 \lesssim \sqrt{d(d+s^*)\log p/n}.$$
 (C.13)

For the second estimated canonical vector \hat{b}_1 , we have

$$||b_{1} - \hat{b}_{1}||_{2} = \left| \frac{B_{*}^{T} a_{1}}{||B_{*}^{T} a_{1}||_{2}} - \frac{\hat{B}^{T} \hat{a}_{1}}{||\hat{B}^{T} \hat{a}_{1}||_{2}} \right||_{2} \lesssim ||B_{*}^{T} a_{1} - \hat{B}^{T} \hat{a}||_{2}$$

$$\leq ||B_{*}^{T} a_{1} - B_{*}^{T} \hat{a}_{1}||_{2} + ||B_{*}^{T} \hat{a}_{1} - \hat{B}^{T} \hat{a}_{1}||_{2}$$

$$\leq ||B_{*}^{T}||_{2} ||a_{1} - \hat{a}_{1}||_{2} + ||B_{*}^{T} - \hat{B}^{T}||_{2} ||\hat{a}_{1}||_{2}.$$
(C.14)

By Assumption 2 and (C.13),

$$||B_*^T||_2 ||a_1 - \hat{a}_1||_2 \lesssim \sqrt{d(d+s^*)\log p/n}.$$
 (C.15)

Note that

$$||B_*^T - \hat{B}^T||_2 \le ||B_*^T - \hat{B}^T||_F = ||B_* - \hat{B}||_F \lesssim \sqrt{\frac{ds^* \log p}{p}},$$
 (C.16)

where the last inequality is because of Lemma C.1. By (C.13), $\|\hat{a}_1\|_2 \leq \|a_1 - \hat{a}_1\|_2 + \|a_1\|_2 \lesssim 1$. Therefore, combining (C.13), (C.14), (C.15) and (C.16) yields

$$||b - \hat{b}||_2 \lesssim \sqrt{d(d+s^*)\log p/n} + \sqrt{\frac{ds^*\log p}{n}} \lesssim \sqrt{d(d+s^*)\log p/n},$$

with probability at least $1 - Cd^2/p$. The results of Theorem 1 follow the union bound inequality. Thus, we finish the proof.

References

Aguet, F., Barbeira, A. N., Bonazzola, R., Brown, A., Castel, S. E., Jo, B., Kasela, S., Kim-Hellmuth, S., Liang, Y., Oliva, M., et al. (2019). The GTEx consortium atlas of genetic regulatory effects across human tissues. *BioRxiv*, page 787903.

- Barry, J. D., Fagny, M., Paulson, J. N., Aerts, H. J., Platig, J., and Quackenbush, J. (2018). Histopathological image QTL discovery of immune infiltration variants. *iScience*, 5:80–89.
- Chen, J., Bushman, F. D., Lewis, J. D., Wu, G. D., and Li, H. (2012). Structure-constrained sparse canonical correlation analysis with an application to microbiome data analysis. *Biostatistics*, 14(2):244–258.
- Chen, M., Gao, C., Ren, Z., and Zhou, H. H. (2013). Sparse CCA via precision adjusted iterative thresholding. arXiv preprint arXiv:1311.6186.
- Friedman, J., Hastie, T., and Tibshirani, R. (2010). Regularization paths for generalized linear models via coordinate descent. *Journal of Statistical Software*, 33(1):1.
- Gao, C., Ma, Z., Zhou, H. H., et al. (2017). Sparse CCA: Adaptive estimation and computational barriers. *The Annals of Statistics*, 45(5):2074–2101.
- Glahn, H. R. (1968). Canonical correlation and its relationship to discriminant analysis and multiple regression. *Journal of the Atmospheric Sciences*, 25(1):23–31.
- González, I., Déjean, S., Martin, P. G., and Baccini, A. (2008). CCA: An R package to extend canonical correlation analysis. *Journal of Statistical Software*, 23(12):1–14.
- Hardoon, D. R. and Shawe-Taylor, J. (2011). Sparse canonical correlation analysis. *Machine Learning*, 83(3):331–353.
- Horn, R. A. and Johnson, C. R. (2012). Matrix Analysis. Cambridge University Press.
- Hotelling, H. (1936). Relations between two sets of variates. Biometrika.
- Lê Cao, K.-A., Martin, P. G., Robert-Granié, C., and Besse, P. (2009). Sparse canonical methods for biological data integration: Application to a cross-platform study. *BMC Bioinformatics*, 10(1):34.
- Lee, W., Lee, D., Lee, Y., and Pawitan, Y. (2011a). scca: Sparse Canonical Covariance Analysis. R package version 1.1.1.
- Lee, W., Lee, D., Lee, Y., and Pawitan, Y. (2011b). Sparse canonical covariance analysis for high-throughput data. Statistical Applications in Genetics and Molecular Biology, 10(1).
- Lutz, J. G. and Eckert, T. L. (1994). The relationship between canonical correlation analysis and multivariate multiple regression. *Educational and Psychological Measurement*, 54(3):666–675.
- Mai, Q. and Zhang, X. (2019). An iterative penalized least squares approach to sparse canonical correlation analysis. *Biometrics*, 75(3):734–744.
- Mardia, K. V., Kent, J. T., and Bibby, J. M. (1979). *Multivariate Analysis*. Johns Hopkins University Press.

- Moll, R., Divo, M., and Langbein, L. (2008). The human keratins: Biology and pathology. *Histochemistry and Cell Biology*, 129(6):705.
- Ning, Y. and Liu, H. (2017). A general theory of hypothesis tests and confidence regions for sparse high dimensional models. *The Annals of Statistics*, 45(1):158–195.
- Parkhomenko, E., Tritchler, D., and Beyene, J. (2007). Genome-wide sparse canonical correlation of gene expression with genotypes. In *BMC Proceedings*, volume 1, page S119. Springer.
- Parkhomenko, E., Tritchler, D., and Beyene, J. (2009). Sparse canonical correlation analysis with application to genomic data integration. Statistical Applications in Genetics and Molecular Biology, 8(1):1–34.
- Pau, G., Fuchs, F., Sklyar, O., Boutros, M., and Huber, W. (2010). Ebimage—an R package for image processing with applications to cellular phenotypes. *Bioinformatics*, 26(7):979–981.
- Peng, C.-Y. and Wu, C. J. (2014). On the choice of nugget in kriging modeling for deterministic computer experiments. *Journal of Computational and Graphical Statistics*, 23(1):151–168.
- Sass, J. O. (2012). Inborn errors of ketogenesis and ketone body utilization. *Journal of Inherited Metabolic Disease*, 35(1):23–28.
- Song, Y., Schreier, P. J., Ramírez, D., and Hasija, T. (2016). Canonical correlation analysis of high-dimensional data with very small sample support. *Signal Processing*, 128:449–458.
- Stein, M. L. (1999). Interpolation of Spatial Data: Some Theory for Kriging. Springer Science & Business Media.
- Stewart, G. W. (1973). Error and perturbation bounds for subspaces associated with certain eigenvalue problems. SIAM Review, 15(4):727–764.
- Tenenhaus, A. and Guillemot, V. (2017). RGCCA: Regularized and Sparse Generalized Canonical Correlation Analysis for Multiblock Data. R package version 2.1.2.
- Tenenhaus, A. and Tenenhaus, M. (2011). Regularized generalized canonical correlation analysis. *Psychometrika*, 76(2):257.
- Tibshirani, R. (1996). Regression shrinkage and selection via the lasso. *Journal of the Royal Statistical Society: Series B (Methodological)*, 58(1):267–288.
- Van Loan, C. F. and Golub, G. H. (1983). *Matrix Computations*. Johns Hopkins University Press.
- Waaijenborg, S., de Witt Hamer, P. C. V., and Zwinderman, A. H. (2008). Quantifying the association between gene expressions and dna-markers by penalized canonical correlation analysis. *Statistical Applications in Genetics and Molecular Biology*, 7(1).

- Wang, Y. R., Jiang, K., Feldman, L. J., Bickel, P. J., Huang, H., et al. (2015). Inferring gene–gene interactions and functional modules using sparse canonical correlation analysis. *The Annals of Applied Statistics*, 9(1):300–323.
- Witten, D. and Tibshirani, R. (2020). *PMA: Penalized Multivariate Analysis*. R package version 1.2.1.
- Witten, D. M., Tibshirani, R., and Hastie, T. (2009). A penalized matrix decomposition, with applications to sparse principal components and canonical correlation analysis. *Biostatistics*, 10(3):515–534.
- Witten, D. M. and Tibshirani, R. J. (2009). Extensions of sparse canonical correlation analysis with applications to genomic data. *Statistical Applications in Genetics and Molecular Biology*, 8(1):1–27.
- Yamamoto, H., Yamaji, H., Fukusaki, E., Ohno, H., and Fukuda, H. (2008). Canonical correlation analysis for multivariate regression and its application to metabolic fingerprinting. *Biochemical Engineering Journal*, 40(2):199–204.

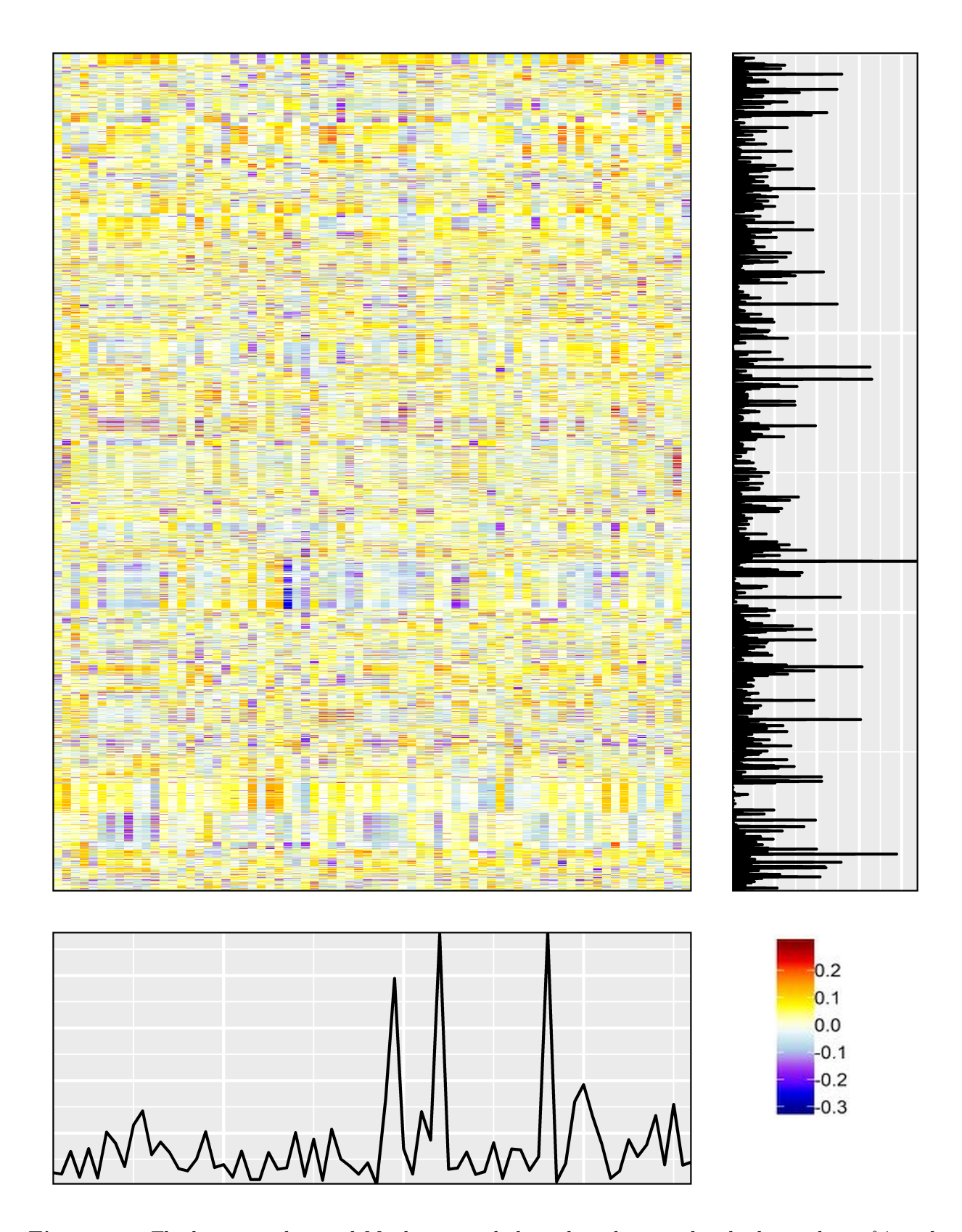


Figure 10: The heatmap plots and Manhattan-style line plots showing the absolute values of \hat{a} and \hat{b} , in which SNPs (rows) and genes (columns) are ordered by genomic position.